Quaternary Science Reviews 225 (2019) 106023

Contents lists available at ScienceDirect

Quaternary Science Reviews

journal homepage: www.elsevier.com/locate/quascirev

A multiproxy record of palaeoenvironmental conditions at the Middle Palaeolithic site of Abric del Pastor (Eastern Iberia)

Rory Connolly [a, b, *], Margarita Jambrina-Enríquez [a], Antonio V. Herrera-Herrera [a], Paloma Vidal-Matutano [c, d], Ana Fagoaga [e, f], Rafael Marquina-Blasco [e, f], María Dolores Marin-Monfort [g], Francisco Javier Ruiz-Sánchez [e, f, h], César Laplana [i], Salvador Bailon [j, k], Leopoldo Pérez [l, m], Lucia Leierer [a, b], Cristo M. Hernández [b], Bertila Galván [b], Carolina Mallol [a, b]

[a] Instituto Universitario de Bio-Organica Antonio Gonzalez (IUBO), Universidad de La Laguna, 38206, Canary Islands, Spain
[b] Departmento de Geografia e Historia, Universidad de La Laguna, 38200, Canary Islands, Spain
[c] TARHA Research Group, Department of Historical Sciences, Universidad de Las Palmas de Gran Canaria, 35003, Canary Islands, Spain
[d] Université Côte-d'Azur, CEPAM, CNRS, France
[e] Grup d'Investigació en Paleontologia de Vertebrats Cenozoics (PVC-GIUV), Àrea de Paleontologia, Universitat de València, Dr. Moliner, 50, CP, 46100, València, Spain
[f] Museu València d'Història Natural, L'Hort de Feliu, P.O. Box 8460, Alginet, València, 46018, Spain
[g] Museo Nacional de Ciencias Naturales (CSIC), José Gutiérrez Abascal 2, 28006, Madrid, Spain
[h] Universidad Estatal Península de Santa Elena, INCYT-UPSE, 7047, Santa Elena, Ecuador
[i] Museo Arqueológico Regional de la Comunidad de Madrid, Pza. Bernardas S/n, 28801, Alcalá de Henares, Spain
[j] Histoire Naturelle de l'Homme Préhistorique, UMR 7194, Sorbonne Universités, MNHN, CNRS, 1, Rue René-Panhard, 75013 Paris, France
[k] Archéozoologie, Archéobotanique: Sociétés, Pratiques, Environnements, UMR 7209, Sorbonne Universités, MNHN, CNRS, 55, Rue Buffon, CP, 55, 2175005, Paris, France
[l] Institut Català de Paleoecologia Humana I Evolució Social (IPHES), Zona Educacional 4. Campus Sescelades URV (Edifici W3), 43007, Tarragona, Spain
[m] Universitat Rovira I Virgili (URV), Área de Prehistoria, Avinguda de Catalunya, 35, 43002, Tarragona, Spain

ARTICLE INFO

Article history:
Received 23 April 2019
Received in revised form
26 September 2019
Accepted 21 October 2019
Available online xxx

Keywords:
Pleistocene
Middle palaeolithic
Europe
Iberia
Neanderthals
Archaeology
Palaeoenvironment reconstruction
Soil micromorphology
Lipid biomarkers
Stable isotopes

ABSTRACT

This paper presents a multiproxy palaeoenvironmental study from Abric del Pastor (Alcoy, Spain), a rock shelter which has yielded evidence for Middle Palaeolithic human occupation. The sedimentary sequence has been analysed for lipid biomarker *n*-alkane abundances (ACL, CPI), compound specific leaf wax δ^2H and $\delta^{13}C$, and bulk organic geochemistry (TOC, %N, %S), providing a record of past climate and local vegetation dynamics. Site formation processes have been reconstructed through the application of soil micromorphology. Analyses of anthracological, microvertebrate and macrofaunal assemblages from selected subunits are also presented here. Our data indicates that a variable climate marked by predominantly cold conditions persisted through most of the sequence and that Neanderthal occupations in stratigraphic unit IVd, assigned to MIS 4 or late MIS 5, occurred in a landscape setting characterised by a mosaic of biotopes. The presence of key resources inside the ravine where the site is located suggests that the occupation of the rock shelter may have been strategically motivated by a subsistence and mobility strategy which focused on zones of localised ecological resilience, such as intra-mountainous valleys or ravines, during periods of global or regional environmental downturn.

* Corresponding author. Instituto Universitario de Bio-Organica Antonio Gonzalez (IUBO), Universidad de La Laguna, 38206, Canary Islands, Spain.
E-mail addresses: rconnoll@ull.es (R. Connolly), mjambrin@ull.edu.es (M. Jambrina-Enríquez), avherrer@ull.edu.es (A.V. Herrera-Herrera), paloma.vidal@ulpgc.es (P. Vidal-Matutano), ana.fagoaga@uv.es (A. Fagoaga), rafael.marquina@uv.es (R. Marquina-Blasco), dores@mncn.csic.es (M.D. Marin-Monfort), francisco.ruiz@uv.es (F.J. Ruiz-Sánchez), cesar.laplana@gmail.com (C. Laplana), salvador.bailon@mnhn.fr (S. Bailon), ljperez@iphes.cat (L. Pérez), lleierer@ull.es (L. Leierer), chergomw@gmail.com (C.M. Hernández), bgalvan@ull.es (B. Galván), cmallol@ull.edu.es (C. Mallol).

https://doi.org/10.1016/j.quascirev.2019.106023

1. Introduction

Abric del Pastor, Alcoy, Spain (Fig. 1) hosts a sequence containing Upper Pleistocene deposits overlain by reworked Holocene sediments. The site has yielded evidence for multiple short-term Neanderthal occupation events (Machado et al., 2013). Archaeological remains recovered from the site include lithic artefacts (Galván Santos et al., 2007; Hernández et al., 2010; Machado et al., 2013), charcoal (Vidal-Matutano et al., 2015, 2017) and faunal remains (Sanchis et al., 2015; Pérez et al., 2017). In addition, at least 17 combustion features have been identified throughout the sequence. Ongoing excavations have produced a sedimentary sequence which has been divided into six primary lithostratigraphic units (S.U. I - VI), with further subdivisions therein. The current chronological framework is based on ESR dates obtained from animal teeth recovered in S.U. IVb (48 kya ±5000 1σ) and S.U. VI (62 kya ±12,000 1σ), as well as an OSL date from a quartz grain recovered in S.U. IVd (63 kya ±5000 1σ) (Mallol et al., 2019) (Fig. 2) (further information on the methods used for dating is provided in the supplementary material, SI Tables 1 and 2). Taking into consideration the error ranges, these dates frame the sequence at Abric del Pastor between 43 kya and 72 kya, covering the whole of

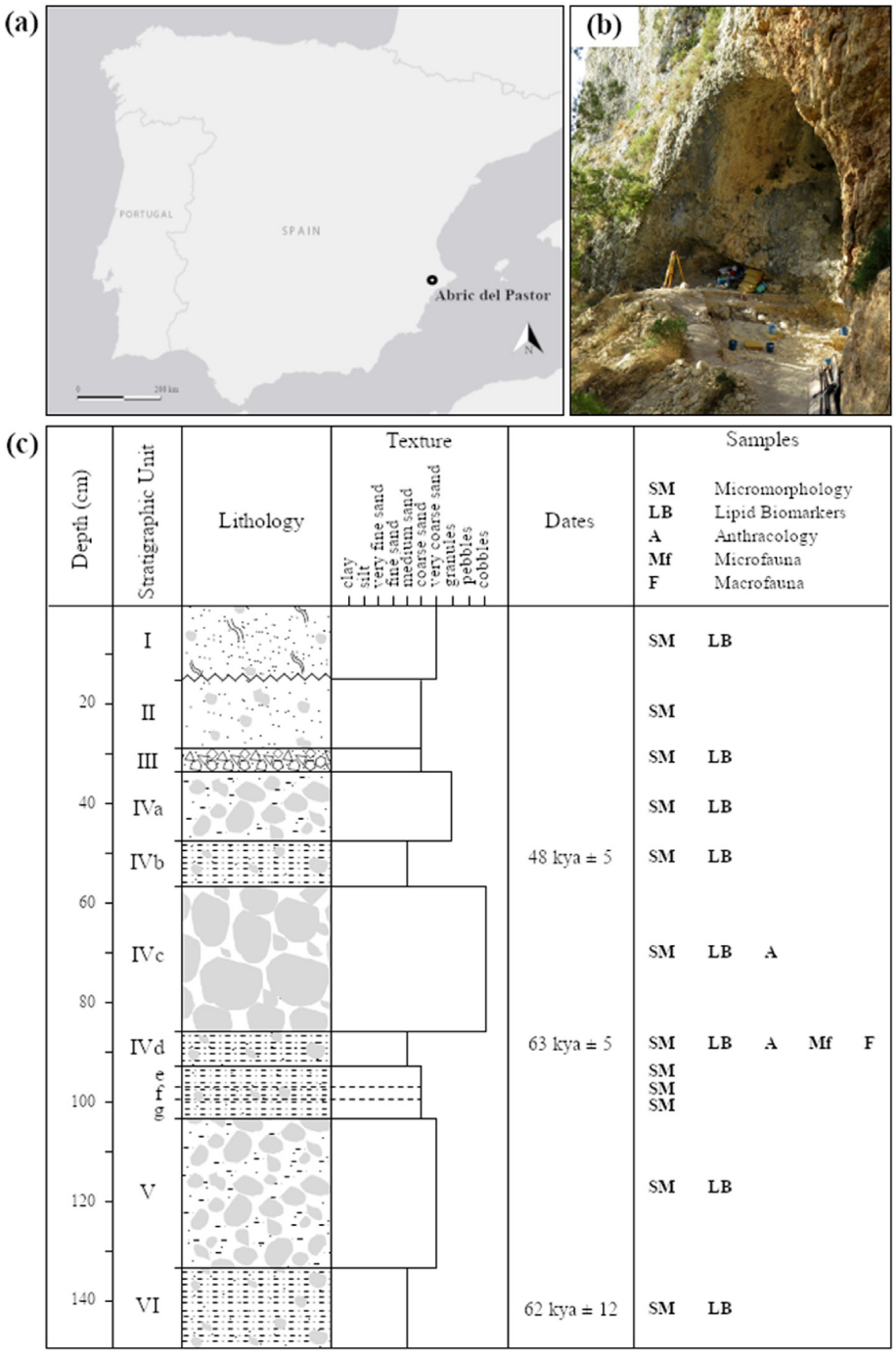

Fig. 1. Location of site (a), drone image of the rock shelter (b) and stratigraphic log showing the sampling locations for the different proxies used in the current study (c). Dates are reported at the one sigma (1σ) confidence level.

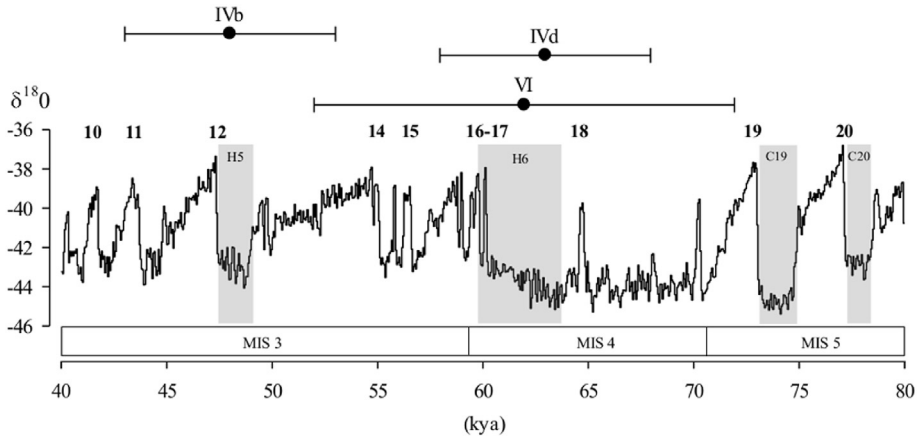

Fig. 2. Comparing the site chronology from Abric del Pastor (S.U. IVc, IVd and S.U. VI, error bars report the one sigma (1σ) confidence level) with δ18O record of the NGRIP ice core (North Greenland Ice Core Project members 2004). ESR (IVb and VI) and OSL (IVd) dates are plotted above. Grey bars indicate the ice-rafting events: H5 – H6 and C19 – C20. Numbers 10 to 20 represent D-O interstadials (Sánchez Goñi et al., 2008; Chapman and Shackleton, 1999).

MIS 4 and potentially extending into late MIS 5 and/or early MIS 3. Although the current dates are stratigraphically coherent, additional samples are required to corroborate the site chronology. With this in mind, our aim here is to provide independent climatic and environmental data, recovered from deposits containing direct evidence for human occupations, against which future hypotheses concerning the chronology of the site and Neanderthal responses to climate change can be further tested.

The Iberian Peninsula is widely regarded as crucial for understanding how Neanderthals responded to fluctuations in environmental conditions (Jiménez-Espejo et al., 2007; Wood et al., 2013; Marín-Arroyo et al., 2018), and the prospect of an MIS 4 setting for the occupations recorded in S.U. IVd warrants consideration, as the palaeoenvironmental record for this marine isotope stage in the Iberian Peninsula remains poorly resolved in comparison to MIS 5 (e.g. Blain et al., 2014; Torres et al., 2015; Daura et al., 2015; Ochando et al., 2019) or MIS 3 (e.g. d'Errico and Sánchez Goñi, 2003; Blain et al., 2013; López-García et al., 2014; Sánchez-Hernández et al., 2014; Alcaraz-Castaño et al., 2017; Daura et al., 2017). There is a paucity of long-term continuous terrestrial sequences and site-specific records for the peninsula, although offshore marine records suggest that rapid global climatic cooling and a significant decrease in sea-surface temperatures (SST) may have driven the development of semi-desert vegetation (Sánchez Goñi et al., 1999; Sánchez Goñi and d'Errico, 2005). The peninsula, owing to its latitudinal range, its diverse topography and the climatic influence of the Atlantic Ocean and Mediterranean Sea, is characterised by considerable climatic diversity in which local environmental conditions change abruptly over relatively short distances (Rivas-Martínez, 1987; López-García et al., 2013). In this context, localised zones of ecological resilience (Holling, 1973; Gunderson, 2000), or vegetation refugia, may have provided conditions favourable to human occupation and subsistence during periods of global climatic deterioration.

New evidence and site-specific environmental records are required to improve our understanding of the role which climate may have played in Neanderthal social and cultural evolution. From this perspective, we investigate carbon and hydrogen isotope values of individual lipid biomarkers (*n*-alkanes) to gain insight into hydroclimatic and vegetation dynamics through the stratigraphic sequence at Abric del Pastor (S.U. I–VI; 110 cm). These proxies are now widely used for palaeohydrological and palaeoecological reconstructions (Bi et al., 2005; Sachse et al., 2012; Collins et al., 2013, 2017; Diefendorf and Freimuth, 2017; Jordan et al., 2017; Norström et al., 2018; Wu et al., 2018). Sedimentary *n*-alkanes are saturated aliphatic hydrocarbons derived from the epicuticular leaf waxes of vascular plants. Plants usually produce *n*-alkanes with a range of different chain lengths and an odd-over-even predominance (Eglinton et al., 1962; Eglinton and Hamilton, 1967). These compounds have been shown to preserve well in sediments and yield valuable information about their biological source, making them well suited for palaeo-ecosystem reconstructions. Compound specific $\delta^{13}C$ and $\delta^{2}H$ of individual *n*-alkanes, which record both ecologic (carbon isotope) and hydrologic (hydrogen isotope) information, are also increasingly being utilised in terrestrial palaeoenvironmental research (Yang and Huang, 2003; Collins et al., 2013, 2017; Jambrina-Enríquez et al., 2016; Uno et al., 2016; Wang et al., 2016; Wu et al., 2018). Different processes govern the carbon and hydrogen isotopic compositions of leaf waxes, thus revealing different information about past environmental conditions.

Among other factors, $\delta^{13}C_{wax}$ values are influenced by the ratio between ^{12}C and ^{13}C in the atmosphere ($\delta^{13}C_{atm}$) and isotopic discrimination during photosynthetic carbon fixation ($\triangle\delta\ ^{13}C$). Studies have demonstrated that differences in ^{13}C fractionation among C3 and C4 plants are recorded by leaf wax $\delta^{13}C$ values, making it possible to discriminate between these vegetation types. Other factors such as water availability, taxa, light intensity, nutrient status and canopy effects also influence $\delta^{13}C_{wax}$ values, to various extents (Diefendorf et al., 2010; Kohn, 2010; Diefendorf and Freimuth, 2017). $\delta^{2}H_{wax}$ values are determined by the relative abundance of hydrogen (H) and deuterium (D) in the source water used by plants during leaf wax synthesis (Sachse et al., 2012). As leaf water ultimately derives from precipitation, compound specific isotope analysis of sedimentary *n*-alkanes can yield useful information about the hydrogen isotopic composition of past precipitation ($\delta^{2}H_{p}$). $\delta^{2}H$ values of mean annual precipitation (MAP) have been shown in certain cases to correlate positively with $\delta^{2}H_{wax}$ values (Sachse et al., 2012). The hydrogen isotopic composition of leaf waxes is also, however, influenced by other factors. Liu and An (2018) identify precipitation $\delta^{2}H$, plant type and evapotranspiration as primary controls over $\delta^{2}H_{wax,}$ while additional factors such as aridity, seasonality, temperature and relative humidity can act as second level or third level controls.

Here, we aim to frame our biomolecular data within a broad reconstruction of site formation processes, which are investigated through the application of soil micromorphology. This approach

also offers the opportunity to identify features or processes at the microstratigraphic scale which may be indicative of certain environmental conditions (Courty, 2001; Courty and Vallverdu, 2001; Nicosia and Stoops, 2017). We also include analyses of anthracological, microvertebrate and macrofaunal assemblages from subunit S.U. IVd. We focus our analyses on S.U. IVd as OSL dating implies a possible MIS 4 setting for the Neanderthal occupations recorded in this subunit.

2. Regional setting and site background

2.1. Abric del Pastor

Abric del Pastor is a rock shelter situated 820 m a.s.l on a north facing slope of the Barranc del Cinc ravine in the Mariola mountain range, Alcoy, south-eastern Spain. The site is located approximately 30 km from the modern coastline, encompassing an area of *c.* 60 m^2 and occurs in a geological context characterised by Miocene Tortonian formations composed of bioclastic calcirudites. The shelter is adjacent to the Serpis river and was formed through phreatic erosional processes acting on a karstic paleotube. Processes of chemical dissolution and mechanical weathering, for instance through repeated freeze-thaw cycles during episodes of climatic cooling, appear to be the primary agents driving the sedimentation at the site through the disintegration of autochthonous limestone.

The first excavations at Abric del Pastor were led by Mario Brotons in 1953. This work focused on the central area of the modern excavation surface. A considerable number of faunal remains and lithic artefacts were recovered (for instance >2400 lithics), however, poor record keeping has rendered these materials devoid of any reliable contextual information. Brotons' excavations affected only a small area and the uppermost layers of the archaeological deposits (S.U. I, II, III), leaving most of the site intact (Galván Santos et al., 2007; Molina et al., 2010). Current excavations, directed by the Universidad de La Laguna, Tenerife, are ongoing since 2005.

2.2. Sedimentary sequence

S.U. I (13–65 cm thickness) is formed by episodic Holocene sedimentation. This unit is composed of heavily bioturbated and reworked humic topsoil yielding Middle Palaeolithic industries alongside diagnostic Neolithic pottery fragments and other modern anthropogenic debris.

S.U. II (08–13 cm thickness) is an isolated pocket of matrix-supported dark brown sandy gravelly sediment truncated by S.U. I at the NW corner of the excavation area. Components include faunal remains and a single combustion feature.

S.U. III (03–12 cm thickness) is a thin, locally discontinuous, partially cemented carbonate crust composed of calcareous sand and fine to medium gravel. This unit has yielded few archaeological remains.

S.U. IV (55–72 cm thickness) is composed of laterally discontinuous, clast-supported, limestone cobble beds (subunits IVa, IVe and IVg) interspersed by loosely compacted, matrix-supported, fine-grained, calcareous sandy-gravelly deposits with frequent limestone cobbles (subunits IVb, IVd and IVf). Subunit IVc, which extends across the whole excavation surface, is composed of boulders and large angular cobbles with very little fine material, resulting from one or more significant roof collapse events. S.U. IV has yielded abundant archaeological material including lithics, faunal remains, combustion features and charcoal. Previous archaeostratigraphic analyses of the lithic record incorporating Raw Material Units (RMU's) and refits has identified between 4 and 6 short-term Neanderthal occupation episodes within subunits IVa, IVb and IVc alone (Machado et al., 2013).

S.U. V (15–25 cm thickness) is notable for a concentration of large boulders in the SW part of the excavation surface, representing a partial collapse of the shelter roof. The bulk of the deposit is composed of loosely compacted, matrix-supported, fine-grained calcareous sand with fine to medium gravel.

S.U. VI (indeterminate thickness) is composed of moderately compacted sandy-silty sediment with a relatively low proportion of small and medium gravel. Despite excavation of this unit having so far been limited to the 4 m^2 sondage situated at the back of the rock shelter (supplementary figure SF 1), a dense concentration of combustion residues, lithics and faunal remains have been recorded.

3. Material and methods

Bulk sediment samples representing S.U.'s I, III, IV, V and VI were collected in vertical sequence from the north profile (A7[1], Z7[2], see supplementary figure SF 1). S.U. II has not been analysed for lipid biomarkers or organic geochemistry as this is a discreet unit only present in a small pocket at the NW corner of the excavation surface. All samples were collected using stainless steel spatulas washed with MeOH and dichloromethane (DCM), using Al foil to avoid phthalate contamination from plastic bags. Samples were then stored at −20 °C and subsequently sub-sampled for lipid biomarker analyses and organic geochemistry.

3.1. Total organic carbon (TOC), % sulphur (%S), % nitrogen (%N)

TOC and %S was analysed with a LECO SC 144DR furnace. Measurement accuracy is 1% RSD *or* ± 25 ppm for carbon (RMS 0.053648) and 1% RSD *or* ± 2.5 ppm for sulphur (RMS 0.044829). %N was measured using a VARIO MAX CN elemental analyser. The standard deviation is <0.3% and the rate of recovery >99.5%. Analyses were carried out at the Instituto Pirenaico de Ecología (IPE-CSIC), Spain.

3.2. Extraction and analysis of n-alkanes

Extraction and analyses of lipids as well as subsequent isotopic analyses of all samples were carried out at the Archaeological Micromorphology and Biomarkers Laboratory (AMBI), Universidad de La Laguna, Tenerife. 20 g sediment samples were dried at 60 °C for 48 h and subsequently ground and homogenised using an agate pestle and mortar which had been cleaned with MeOH and dichloromethane (DCM). All non-volumetric glassware used for lipid extraction were thoroughly cleaned, solvent washed with MeOH and calcined at 450 °C for 10 h prior to extraction to eliminate potential contaminants. Lipids from 20 g sediment samples were extracted in 150 mL dichloromethane/methanol (DCM:MeOH 9:1) by ultrasonic extraction (three cycles of 30 min) and centrifugation (three cycles at 4700 rpm). The total lipid extract (TLE) was then concentrated under a steady flow of N_2 gas at 40 °C in a rotary evaporator. The TLE was subsequently reconstituted using DCM and separated into fractions of differing polarity by solid phase extraction (SPE) through a silica gel column (1 g silica, 70–230 mesh and 0.1 g sand 50–70 mesh, both previously calcined at 450 °C for 10 h).

Here we present results of fraction 1 (F1: *n*-alkanes), which was eluted with $^3/_8$ of dead volume (DV) in *n*-hexane. F1 was subsequently concentrated under a steady stream of N_2 gas at 40 °C in an Organomation rotary evaporator and stored at −20 °C. Prior to measurement, 3 μL of internal standard (IS) 5α-androstane 8 mg/L was added and the volume was completed with 150 μL of DCM. F1

was analysed by gas chromatography with a coupled detection and mass-selective detector (GC-Agilent 7890B, MSD Agilent 5977A) equipped with a HP-5MS capillary column (30 m, ID: 250 μm, film thickness 0.25 μm). A temperature program was applied with an initial temperature of 70 °C for 2 min and a heating rate of 12 °C/min to 140 °C, and a final temperature of 320 °C with a heating rate of 3 °C/min for 3 min, using a Helium carrier gas (2 ml/min). The PVT injector was held at a split ratio of 5:1 at an initial temperature of 70 °C for 0.85 min and heated to 300 °C at a programmed rate of 720 °C/min.

Compounds were identified by comparison of their retention times and mass spectra to those of reference compounds (mix C_8—C_{40} and 5α-androstane, Supelco) and mass spectral library databases (NIST). Analytes were quantified using calibration curves obtained by plotting the ratio Area/$Area_{IS}$ *versus* the concentration of each reference compound, with correlation coefficients higher than 0.995. The *n*-alkane concentration is expressed as μg of individual compound per gram of dry sample (μg gds^{-1}). Error ranges for individual *n*-alkanes are reported as standard deviation (SI Table 3).

To evaluate the distribution of *n*-alkanes we used the average carbon length (ACL) and carbon preference index (CPI). Indices such as ACL and CPI yield important information on the potential sources of sedimentary OM. ACL values, which are broadly structured by phylogenetic relationships, reflect changes in vegetation structure through a sedimentary sequence. Temperature and hydrological controls, however, also play a role in determining ACL values within individual plant communities (Sachse et al., 2006; Diefendorf et al., 2015a). CPI values are related to the odd-over-even predominance (OEP) of *n*-alkanes, where values > 5 have typically been associated with epicuticular wax of higher plants and lower values ~1 with bacteria or algae (Cranwell et al., 1987). CPI has also been employed as an indicator of *n*-alkane degradation in sediments, where low temperatures and dry conditions correspond to low diagenetic rates resulting in increased CPI values, and increased temperatures with more humid conditions correspond to higher diagenetic rates and lower CPI values (Kuder and Kruge, 1998; Xie et al., 2004; Ortiz et al., 2010). CPI values vary considerably within and amongst different plant species, however, so a cautious approach should be taken to the use of CPI as a quantitative indicator of *n*-alkane degradation (Bush and McInerney, 2013). CPI values can also be affected by thermal degradation through the incorporation of charred biomass (Eckmeier and Wiesenberg, 2009; Wiesenberg et al., 2009; Diefendorf et al., 2015b; Wang et al., 2017). As such, these values are best interpreted in conjunction with other proxies.

The ACL metric, originally defined by Poynter et al. (1989), was calculated here following the recommendations of Freeman and Pancost (2013) using the C_{18} - C_{35} interval:

$$ACL_{18-35} = \sum(Ci \times [Ci]) / \sum[Ci];\ 18 \le i \le 35$$

The CPI value (C_{18} to C_{35}) was calculated following the equation set out in Bray and Evans (1961):

$$CPI_{18-35} = [(\sum C_{19-35odd} / ? \sum C_{18-34even}) + (\sum C_{19-35odd} / \sum C_{20-36even})] \times 0.5$$

3.2.1. Gas chromatography — isotope ratio MS (GC-IRMS)

Carbon and hydrogen isotope analysis of individual *n*-alkanes was carried out using a Thermo Scientific Isotope Ratio Mass Spectrometer Delta V Advantage coupled to a GC Trace1310 through a Conflo IV interface with a temperature converter GC Isolink II. The GC was fitted with a Trace Gold 5-MS (Thermo Scientific) fused silica capillary column ((5%-diphenyl)-dimethylpolysiloxane, 30 m length x 0.25 mm i.d., 0.25 μm film thickness). Helium was used as the carrier gas at a flow rate set at 1.5 mL/min. All measurements were repeated three times. Data acquisition and processing were carried out using the Isodat 3.0 software (Thermo Scientific).

Carbon and hydrogen isotope values are reported for *n*-alkanes C_{29} and C_{31} because these compounds were consistently present in sufficient concentrations for isotopic analyses. Samples were injected by means of a Programmed Temperature Vaporising injector (PTV) in splitless mode, with the temperature increasing from 60 °C to 79 °C (held 30 s, rate 10 °C/min), then to 325 °C (held 3 min) at a rate 10 °C/s and finally to 350 °C (held 3 min) at 14 °C/s. The temperature programme comprised a 2 min isothermal period at 70 °C increasing to 140 °C (held 2 min) at a rate of 12 °C/min, followed by an increase period to 320 °C (held 15 min) at 3 °C/min. Combustion reactor temperature was maintained at 1000 °C for carbon isotope analysis. The high temperature conversion (HTC) oven was maintained at 1420 °C for hydrogen isotope analysis. Obtained values were normalised to the Vienna Pee Dee Belemnite (VPDB) scale ($\delta^{13}C$) and Vienna Standard Mean Ocean Water (VSMOW) scale ($\delta^{2}H$) using a *n*-alkane Schimmelmann type A6 mixture (*n*-C_{16} to *n*-C_{30}) of known isotopic composition from Arndt Schimmelmann (Biogeochemical Laboratories, Indiana University). Certificate of analysis indicates that data for *n*-alkane Schimmelmann type A6 mixture have a precision of ±0.05‰ for $\delta^{13}C$ and ±1.5‰ for $\delta^{2}H$. Reproducibility was better than ±0.5‰ for carbon isotope measurements and better than ±5.0‰ for hydrogen isotope measurements.

To investigate the processes governing the hydrogen composition of sedimentary *n*-alkanes, a robust dataset of the isotopic signatures of potential sources, such as precipitation, is required. Here we consider monthly precipitation amount and precipitation $\delta^{2}H$ ($\delta^{2}H_p$) data available from two GNIP stations near the study area for comparison (Global Network for Isotopes in Precipitation; IAEA/WMO, 2006).

3.3. Micromorphology

Intact, oriented blocks of sediment from all stratigraphic units were extracted from selected profiles and from across the excavation surface for micromorphological analyses. The goal of applying this technique was to characterise site formation processes and to identify features or processes at the microstratigraphic scale which could be indicative of particular climatic or environmental conditions.

Samples were oven dried at 60 °C for 48 h and subsequently impregnated with a mixture of polyester resin (Palatal strained resin UN1866, TNK composites), styrene (Styrene monomer [CAS: 100-42-5] UN2055, TNK composites) and catalyzer (Luperox [CAS: 78-93-3], TNK composites) in a 7:3:0.1 ratio. The hardened blocks were then cut in 1 cm-thick slabs using a Euro-Shatal M31100 radial saw. Samples collected during archaeological field seasons 2010—2015 were sent to Spectrum Petrographics (Vancouver, WA, USA) for thin section manufacture (7 cm × 5 cm x 30 μm). Samples collected during the 2016—2018 field seasons were processed at the Archaeological Micromorphology and Biomarker Laboratory (AMBI), Universidad de La Laguna, Tenerife. Micromorphological analyses were carried out using a Nikon E200 polarising microscope following the standard guidelines set out in Stoops (2003) and Nicosia and Stoops (2017).

3.4. Anthracology

During the archaeological field seasons carried out between

2013 and 2016 the sediment excavated from across the entire excavation surface of S.U. IVc and S.U. IVd was processed by systematic flotation using 1.0 and 0.2 mm sieves. S.U. IVd is subdivided into IVd1, IVd2, IVd3, IVd4 and IVd5, which represent distinct, locally discontinuous textural facies assigned during excavation of this unit. In this paper, scattered charcoal from these units are included, excluding the concentrated charcoal from the combustion features. Scattered charcoal spread over human living surfaces, having accumulated from an undefined number of combustion and occupation events, are widely accepted as reflecting conditions within the local environment (Badal and Heinz, 1991; Badal, 1992; Chabal, 1997).

For the taxonomic identification of specimens, each fragment of charcoal was fractured manually to provide transversal, tangential and radial sections using a Nikon Optiphot-100 bright/dark field incident light microscope with 50–500x magnification. Botanical identification was performed with specialised plant anatomy atlases (Jacquiot et al., 1973; Schweingruber, 1976, 1990) as well as the reference collection of modern charred woody taxa from the Department of Prehistory, Archaeology and Ancient History, University of Valencia. Spatial information relating to the current distribution of taxa has been obtained from the database of the Anthos Project (www.anthos.es) and processed using GIS software (Quantum GIS v.2.10.1 "Pisa").

3.5. Microvertebrate study (S.U. IVd)

3.5.1. Microvertebrate remains

The small vertebrate fossil remains studied in this work consist of isolated dental and bone fragments collected during the 2013 archaeological field season from S.U. IVd, across the excavation surface. The fossils were processed, sorted and classified using a Leica MS5 binocular microscope. Photographs were taken with a scanning electron microscope at Central Support Facility for Experimental Research (SCSIE) of the Universitat de València. Vertebrate fossils were identified following the anatomical nomenclature and measurement methods provided by van der Meulen (1973), Rabeder (1981) and Jeannet (2000) for arvicolines, van der Weerd (1976) for murids, Daams (1981) for glirids, Reumer (1984) for soricids, Bailon (1999) for amphibians, Roček (1984), Bailon (1991), Barahona (1996) and Barahona and Barbadillo (1997) for lacertids and Szyndlar (1984) and Blain (2009) for snakes. The taxonomic classification follows Wilson and Reeder (2005) for mammals, Uetz and Hošek (2015) for reptiles and Frost (2015) for amphibians.

3.5.2. Palaeoecological reconstruction (microvertebrates)

To reconstruct the climatic conditions of S.U. IVd, the Mutual Ecogeographic Range (MER) method has been applied to the assemblage (Blain et al., 2009, 2016). This consists of identifying regions where the recorded species are currently found and extrapolating the current mean values of the climatic parameters of these regions as representative climate estimations for the studied site. This procedure suggests avoiding those species whose distribution is strongly affected by perturbing parameters, such as human pressure. Hence, *Microtus cabrerae*, taxon registered in S.U. IVd, has not been included in this study because it has suffered a range contraction in modern times and many subpopulations are small, fragmented and subject to major inter-annual fluctuations (Laplana and Sevilla, 2013; Pita et al., 2014). Biogeographic cartography of small mammal species in Spain, recorded as presence/absence of each taxa in a 10×10 km UTM square grid, was obtained from Palomo et al. (2007), while amphibians and reptiles came from SIARE (AHE, 2016). Climatic information (MAT, mean annual temperature; MAP, mean annual precipitation; MTW, maximum temperature of warmest month; MTC, minimum temperature of coldest month; PWM, precipitation of wettest month; PDM, precipitation of driest month) for these locations was obtained from the World Clim 1.4 database with a 30 arcseconds resolution grid (Hijmans et al., 2005). The resulting climatic parameters were compared with the current climate data from the nearest weather station to the site (Alcoy). Further details of the methods employed for the microvertebrate study and taphonomic remarks on the assemblage are given in the supplementary material.

3.6. Macrofaunal study (S.U. IVd)

3.6.1. Zooarchaeological methods

Zooarchaeological and taphonomic analyses of faunal material recovered during the excavation of S.U. IVd were performed using established standard methods (Lyman, 1994; Reitz and Wing, 2008). Where present, material was recorded for all excavation squares across the excavation surface. Remains were taxonomically and anatomically identified, except in specimens with insufficient information. Those remains were classified into three categories (long, flat or articular) and associated with a weight-size category based on bone density, circumference and the thickness of the cortical surface. Weight-size categories were determined in keeping with archaeological examples (Uerpmann, 1973; Bunn, 1986) and current weight references based on wild male specimens (Palomo et al., 2007): large-sized (>300 kg), medium-sized (100–300 kg), small-sized (5–100 kg) and very small-sized (<5 kg). Five abundance measures were employed: number of remains (NR), number of identified specimens (NISP), the minimal number of elements (MNE), the minimal number of individuals (MNI) and the minimal animal units (MAU). To assess the integrity of the assemblage, we calculated the fragmentation rate, the relative abundance (%RA) and the standardized MAU (%MAU). The last of these was used to calculate the differential preservation index by weight-size, applying the Pearson's r and Kendall's tau correlation coefficient test with Past 3.12© free software. Published data was referred to for large and medium-sized animals (Kreutzer, 1992; Lam et al., 1999) and for small-sized animals (Lyman, 1984, 1985; 1994). Further information on the methods used for the study of the macrofaunal material is provided in the supplementary material.

3.6.2. Palaeoecological reconstruction (macrofauna)

The formalisation of indicator species according to a bioclimatic classification has been applied here (Hernández-Fernández, 2001; Rodríguez, 2013; Walter, 1973). A table has been constructed with the theoretical distribution of species according to different biomes or Climate Restriction Index (CRI). The distribution in the reference material is established for mammalian species, in our work we have also included the theoretical distribution of other taxa registered in the set, i.e. birds and tortoises. Once the CRI is calculated, the bioclimatic component (BC) of the set for each biome is obtained by means of the formula $BC = (\Sigma CRIi) * 100/S$, where S is the number of species and CRIi the index of climatic restriction of each of the species. Previously calculated discriminant functions are applied from a wide database of localities and species (Hernández-Fernández, 2001, 2006; Hernández-Fernández and Peláez-Campomanes, 2003), in order to obtain data such as annual average temperature (AAT) or precipitation (AAP). From this, it is possible to infer the most probable biome for our faunal assemblage (Pérez et al., 2017).

4. Results

4.1. Total organic carbon (TOC), % sulphur (%S), % nitrogen (%N)

TOC ranged from 0.06 to 3.91% with an average of 1.11% (Fig. 3). The highest concentration was recorded in the uppermost part of S.U. I, while the lowest concentration of TOC was recorded in S.U. V. Mild fluctuations and a generally decreasing trend is observed down-profile, with the exception of S.U VI, where there is a slight increase of 0.8%. TS values ranged between 0.01% and 0.07%, with an average value of 0.03% (Fig. 3). The maximum concentration of TS, 0.07%, is recorded in the uppermost part of S.U I. The lowest values for TS are recorded in S.U. IVc and IVd. TN values ranged from 0.01% to 0.29%, with an average TN value through the sequence of 0.07% (Fig. 3). The maximum value of 0.29% is recorded as a sharp increase in the lower part of S.U. I. Mild fluctuations are observed down-profile between 0.01% and 0.03%.

4.2. Sedimentary leaf waxes

4.2.1. Distribution of n-alkanes

Total *n*-alkane concentration ranged between 0.04 and 1.59 μg/g dry sediment. Most samples through the sequence yielded *n*-alkane distributions with a predominance of long chain compounds (C_{29}–C_{35}), consistent with higher order vascular terrestrial plants (Fig. 4) (Table 1), although samples collected from S.U IVc and S.U. IVd also show input from mid-chain length compounds (C_{23}–C_{27}). Even-numbered homologues recorded in S.U. IVb (lower) and S.U. VI were below the limit of quantification, so CPI values for those units are not included here. CPI values through the sequence are generally low, with a minimum of 0.7 (S.U. V) and a maximum of 7.9 (S.U. III) (Fig. 5). ACL values ranged between a minimum of 27.2 (S.U. IVd upper) and a maximum of 32.5 (S.U. V), with a notable shift toward lower values in S.U. IVc and S.U. IVd (upper).

4.2.2. δ^2H_{wax}

In the region around Abric del Pastor, a strong negative correlation between monthly precipitation amount and precipitation δ^2H (δ^2H_p) is recorded at two GNIP (Global Network for Isotopes in Precipitation; IAEA/WMO, 2006) stations in Murcia and Valencia (Fig. 6). This suggests some degree of influence by the amount effect (Dansgaard, 1964) on regional δ^2H_p values, which in turn may contribute to variability in our δ^2H_{wax} signal.

δ^2H_{wax} was analysed for C_{29} and C_{31} *n*-alkanes extracted from sediments collected through the sequence (Fig. 7) (Table 2). For nC_{29}, the δ^2H_{wax} range is −129‰ to −170‰. The lowest values of −170‰ and −164‰ are recorded in the Holocene sediments from S.U. I. A trend towards low values is also recorded in the uppermost part of S.U. IVd and in S.U. IVc, at −152‰ and −153‰ respectively. Through the rest of the sequence values fluctuate between −129‰ and −148‰. δ^2H_{wax} values for nC_{31} are generally lower than those obtained for nC_{29} ranging from −137‰ to −174‰. Overall, however, both sets of values have a similar degree of variation and follow a similar trend.

4.2.3. $\delta^{13}C_{wax}$

$\delta^{13}C_{wax}$ measurements were analysed for C_{29} and C_{31} *n*-alkanes extracted from sediments collected through the sequence (Fig. 7) (Table 2). $\delta13C_{wax}$ values for nC_{29} ranged between −32.4‰ and −38.0‰, with maximum ^{13}C enrichment in S.U. IVb, where values of-32.4‰ and −32.8‰ were obtained. A similarly high value is recorded in the base of S.U. IVd at −32.5‰. The lowest value of −38.0‰ comes from S.U. IVa. $\delta13C_{wax}$ values for nC_{31} are generally lower than those obtained for nC_{29}, ranging between −33.6‰ and −40.3‰. Overall, however, both sets of values have a similar degree of variation and follow a similar trend.

4.3. Micromorphology

4.3.1. Overview

The samples analysed are generally composed of the same sedimentological and lithological elements, characterised by a locally reworked sandy sediment, with 5–10% subangular to angular fine and medium sand, ~30% subrounded coarse sand and gravel, resulting principally from the mechanical weathering and decay of the fossiliferous quartz-rich limestone rock shelter. The

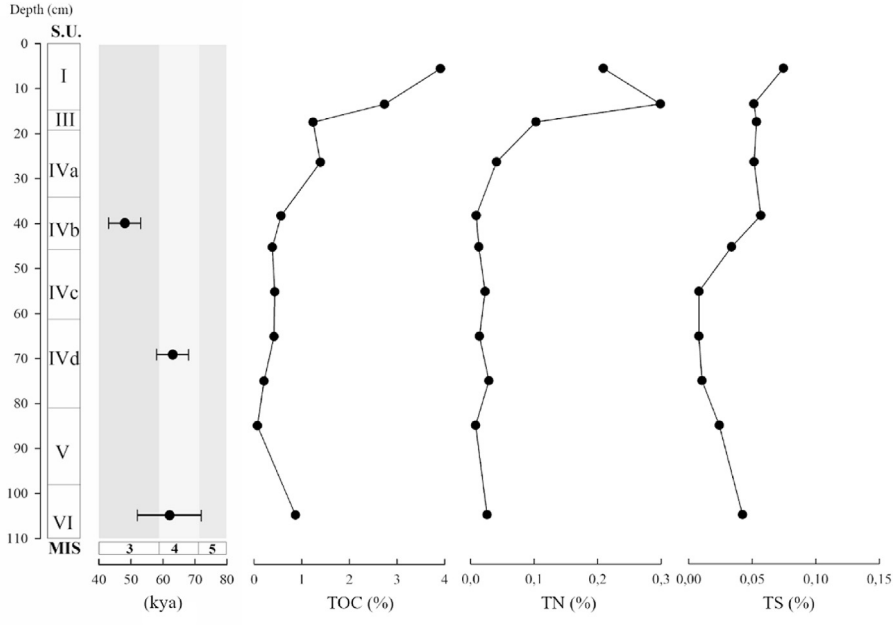

Fig. 3. Total organic carbon (TOC,%), total nitrogen (TN,%), and total sulphur (TS,%).

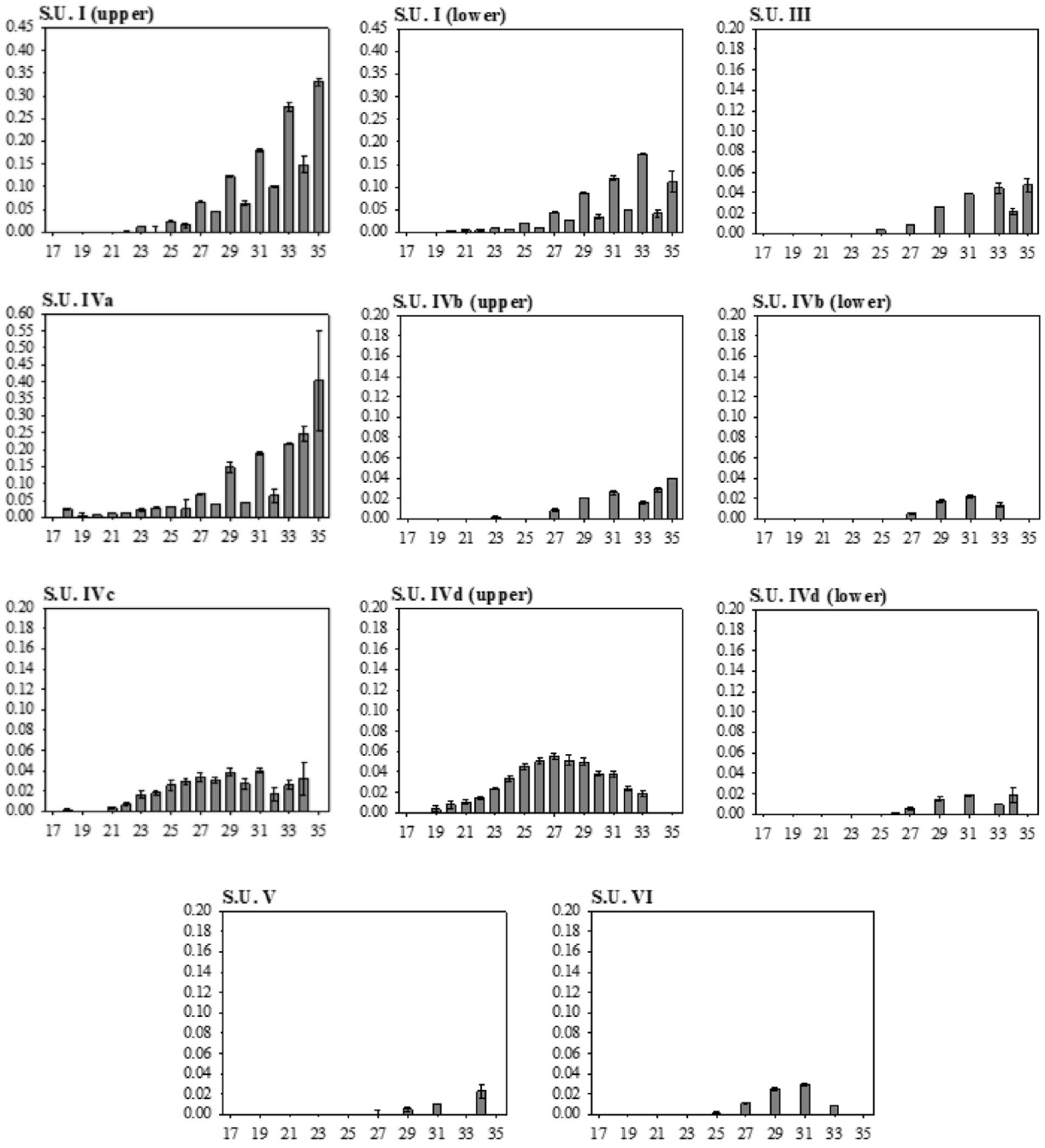

Fig. 4. Histograms displaying the distribution and concentration of *n*-alkanes extracted from sediments at Abric del Pastor. IS: 5α-androstane. The x-axis represents the alkane carbon chain length and the y-axis represents the concentrations given in μg per g of dry sediment (μg/g). Note the larger scale for samples from S.U. I and S.U. IVa.

coarse mineral components frequently appear fissured. The sedimentary matrix is composed of micritic calcite which, with notable exceptions in S.U. IVb and IVd, generally occurs in a good state of preservation with few dissolution features. Clay is present only in small quantities, occurring locally as thin coatings, cappings or infilling the interstitial void space. Detailed descriptions of each thin section sample are provided in a supplementary table (SI Table 5).

4.3.2. Microfacies types

Below, we outline the microfacies types identified through micromorphological analyses of thin sections by polarized light microscopy. Brief descriptions are included with a representative photomicrograph of each of the primary microfacies types (Fig. 8). Similar features and components are recurrent throughout the sequence (Figs. 9 and 10) but vary considerably in their degree of abundance, reworking or post-depositional alteration.

1. Microfacies type 1 This microfacies type is characterised by a crumb to granular microstructure which is quite open, lithologically composed of fine and medium sand-sized grains of quartz alongside micritic and micro-sparitic fossiliferous limestone, which occurs in sizes ranging from fine sand to coarse gravel. Morphologically this fraction appears subrounded to rounded. Frost induced fissuring of larger clasts is observed in addition to the

Table 1
Total organic carbon (TOC), total nitrogen (TN) and total sulphur (TS) as well as *n*-alkane concentrations, ACL and CPI values through the stratigraphic sequence. * denotes compounds which were detected but in quantities below the limit of quantification.

S.U.	I	I	III	IVa	IVb	IVb	IVc	IVd	IVd	V	VI
TOC%	3.91	2.74	1.24	1.39	0.56	0.43	0.42	0.21	0.07	0.87	0.38
TN%	0.21	0.30	0.10	0.04	0.01	0.01	0.02	0.01	0.03	0.01	0.03
TS%	0.07	0.05	0.05	0.05	0.06	0.03	0.01	0.01	0.01	0.02	0.04
n-Alkanes (μg/g dry sediment)											
C_{17}	*	*	*	*	*	*	*	*	*	*	*
C_{18}	*	*	*	0.025	*	*	0.002	*	*	*	*
C_{19}	*	*	*	0.005	*	*	*	0.004	*	*	*
C_{20}	*	0.003	*	0.007	*	*	*	0.008	*	*	*
C_{21}	0.001	0.006	*	0.013	*	*	0.004	0.01	*	*	*
C_{22}	0.001	0.005	*	0.014	*	*	0.007	0.015	*	*	*
C_{23}	0.012	0.011	*	0.022	0.002	*	0.016	0.023	*	*	*
C_{24}	0.001	0.006	*	0.028	*	*	0.018	0.034	*	*	*
C_{25}	0.024	0.021	0.003	0.032	*	*	0.026	0.045	*	*	0.001
C_{26}	0.015	0.011	*	0.025	*	*	0.029	0.05	0.001	*	*
C_{27}	0.066	0.044	0.009	0.069	0.008	0.005	0.034	0.055	0.006	*	0.011
C_{28}	0.046	0.026	*	0.039	*	*	0.03	0.051	*	*	*
C_{29}	0.123	0.087	0.026	0.148	0.021	0.017	0.038	0.05	0.014	0.005	0.025
C_{30}	0.063	0.035	*	0.044	*	*	0.027	0.038	*	*	*
C_{31}	0.181	0.12	0.039	0.188	0.026	0.022	0.04	0.038	0.018	0.011	0.029
C_{32}	0.101	0.049	*	0.064	*	*	0.017	0.023	*	*	*
C_{33}	0.276	0.172	0.044	0.217	0.016	0.014	0.026	0.019	0.012	*	0.009
C_{34}	0.148	0.042	0.021	0.247	0.029	*	0.032	*	0.018	0.023	*
C_{35}	0.331	0.111	0.047	0.403	0.041	*	*	*	*	*	*
Total	1.38	0.75	0.19	1.59	0.14	0.06	0.35	0.46	0.07	0.04	0.07
ACL	32.0	31.1	32.2	31.4	32.3	30.5	28.6	27.2	31.3	32.5	29.9
CPI	2.7	3.3	7.9	2.3	3.9	–	1.1	1.1	2.6	0.7	–

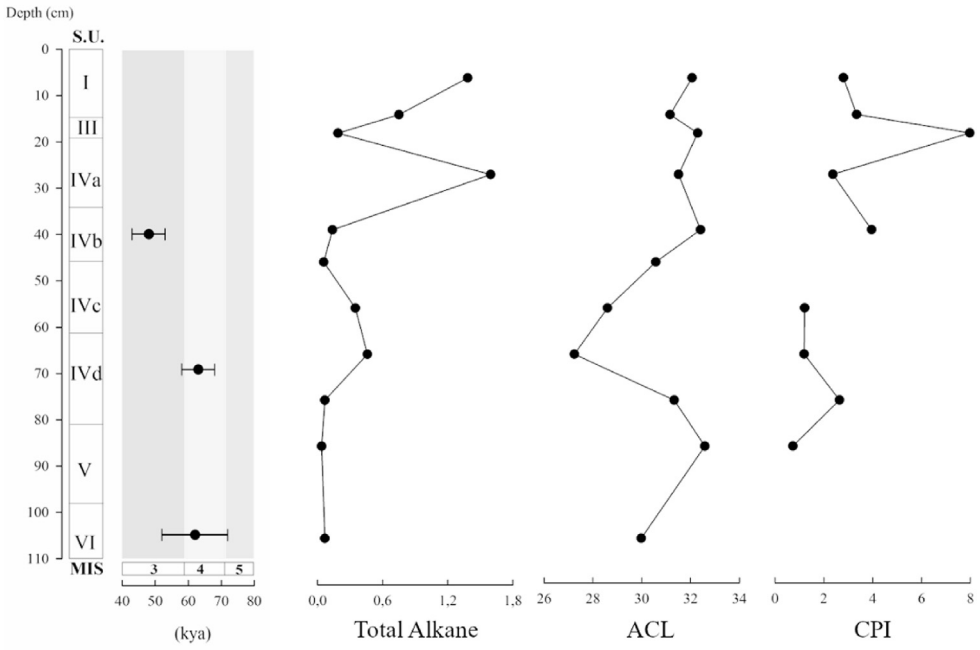

Fig. 5. Leaf wax lipid biomarkers. Total n-alkanes, ACL and CPI.

presence of platy coarse grains. Dusty clay coatings occur throughout, as well as clay cappings. Frequent components include burnt and unburnt angular bone fragments and pieces of both massive and fibrous charcoal, ash rhombs, occasional fat derived char which occurs as ~0.5–1.5 mm massive black fragments with a vesicular porosity, and rare coprolites. The internal organisation of the components is unsorted. This microfacies type is associated with good preservation of the calcitic fraction.

(a) *Microfacies type 1a* This microfacies type is similar to MF type 1 but with a higher degree subrounding and rounding of the coarse mineral elements, Fe–Mn segregation and the presence of limpid clay infillings.
(b) *Microfacies type 1b* This microfacies type is similar to MF type 1a but exhibits a poorer preservation of the calcitic matrix.

2. Microfacies type 2 This microfacies type is characterised by a weakly expressed platy/lenticular microstructure, lithologically

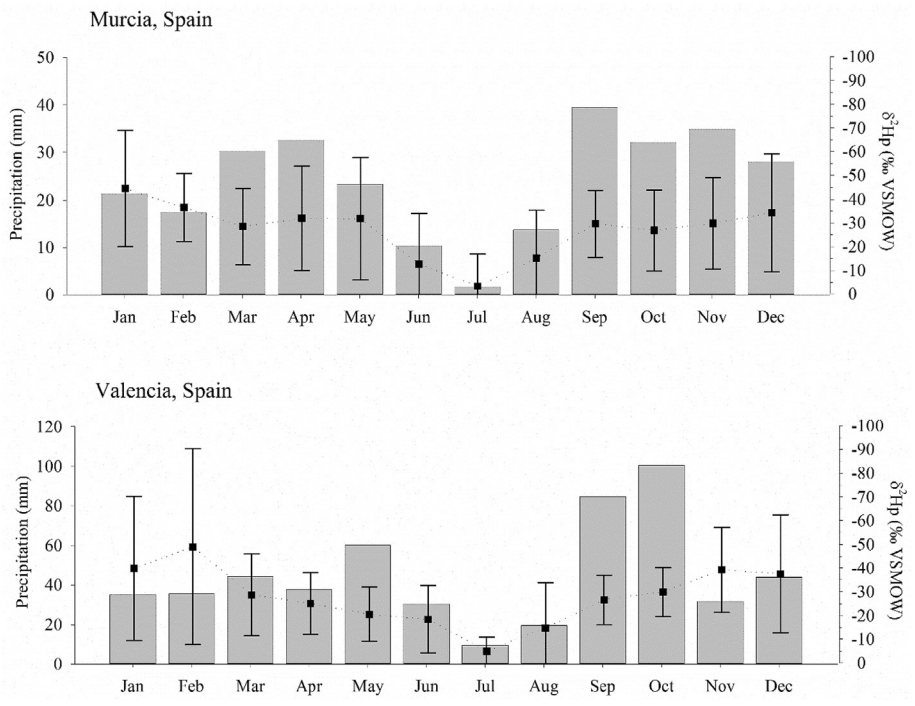

Fig. 6. Seasonal cycle of precipitation amount (grey bars) and δ^2H_p (black squares) for GNIP stations (IAEA/WMO, 2006) in Murcia (n = 11, 2000–2010) and Valencia, Spain (n = 16, 2000–2015).

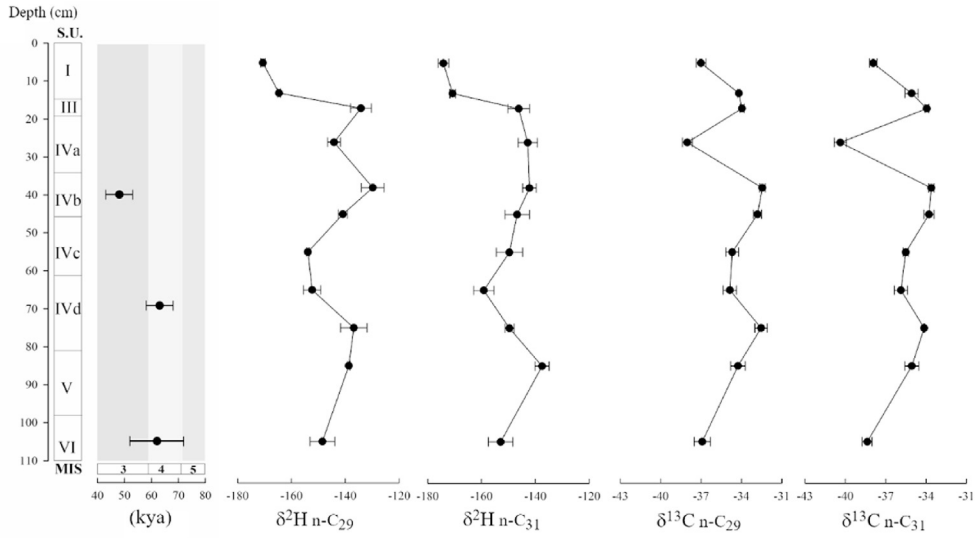

Fig. 7. From left to right; δ^2H_{wax} for n-alkanes C_{29} and C_{31}, and $\delta^{13}C_{wax}$ for n-alkanes C_{29} and C_{31}.

Table 2
δ^2H_{wax} and $\delta^{13}C_{wax}$ through the stratigraphic sequence. Values are expressed in per mil (‰). Error reports standard deviation.

S.U.	I	I	III	IVa	IVb	IVb	IVc	IVd	IVd	V	VI
δ^2H_{wax}											
C_{29}	−170 ± 1	−164 ± 1	−134 ± 4	−144 ± 2	−129 ± 4	−140 ± 2	−153 ± 1	−152 ± 3	−136 ± 5	−138 ± 1	−148 ± 5
C_{31}	−174 ± 2	−170 ± 1	−146 ± 4	−142 ± 4	−142 ± 3	−146 ± 5	−149 ± 5	−159 ± 4	−149 ± 2	−137 ± 3	−152 ± 5
$\delta^{13}C_{wax}$											
C_{29}	−36.9 ± 0.4	−34.2 ± 0.1	−33.9 ± 0.2	−38.0 ± 0.4	−32.4 ± 0.2	−32.8 ± 0.3	−34.7 ± 0.5	−34.9 ± 0.5	−32.5 ± 0.5	−34.3 ± 0.5	−36.9 ± 0.6
C_{31}	−37.9 ± 0.3	−35.1 ± 0.5	−33.9 ± 0.1	−40.3 ± 0.5	−33.6 ± 0.2	−33.8 ± 0.4	−35.5 ± 0.2	−35.9 ± 0.5	−34.1 ± 0.1	−35.1 ± 0.5	−38.4 ± 0.4

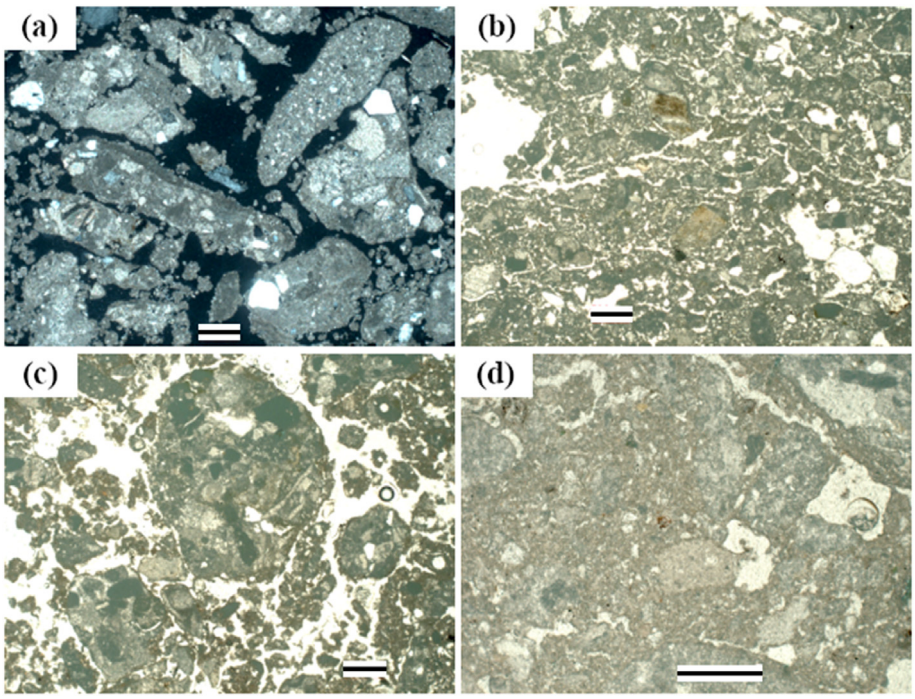

Fig. 8. Photomicrographs of primary microfacies types (scale 500 μm) (a) MF type 1 (b) MF type 2 (c) MF Type 3 (d) MF Type 4.

very similar to MF type 1. Frost induced fissuring of the coarse mineral fraction is again evident. Components include scattered, unsorted, unburnt angular bone fragments and reworked calcitic wood ash. The calcitic fraction is well preserved.

3. Microfacies type 3 This microfacies type is characterised by a spongy to vughy microstructure dominated by a vesicular or vughy porosity. Lithologically this type is composed of fine and medium sand-sized grains of quartz, although in lower abundance than other MF types, alongside micritic and micro-sparitic fossiliferous limestone ranging from fine sand to coarse gravel. Clasts exhibit a high degree of subrounding and rounding. Components are unsorted and scattered and include reworked charcoal and bone. No calcitic wood ash is observed in this MF type. The calcitic fraction is well preserved.

4. Microfacies type 4 This microfacies type is characterised by a massive microstructure with low porosity, and a lithology of fine and medium sand-sized grains of quartz alongside micritic and micro-sparitic fossiliferous limestone ranging in size from fine sand to coarse gravel. Clasts occur as sub-angular to angular. Cryofeatures observed in the other MF types are not as evident here. Components include reworked calcitic ash rhombs and angular unburnt bone fragments. The calcitic fraction is well preserved.

(a) *Microfacies type 4a* This microfacies type is similar to MF type 4 but with subrounded to rounded coarse mineral elements and frost induced fissuring of the coarse grains.

4.3.3. Description

4.3.3.1. S.U. I. This unit is characterised microscopically by MF type 1. The microstructure is crumb to granular with coarse sand and gravel occurring as subrounded to rounded. Organisation of the components is unsorted with a high porosity generated by channels due to root bioturbation. The matrix has a dusty appearance owing to the presence of silt-sized organic matter (humified or carbonised plant cells). Terrestrial snail shell, charcoal, bone fragments and coprolites were identified throughout. Abundant dispersed faecal spherulites were also identified in the uppermost part of this unit.

4.3.3.2. S.U. II. This unit is characterised mainly by MF type 4 but with isolated zones more closely resembling MF type 1. It exhibits a slight increase in the relative proportion of fine and medium sized quartz sand. Medium and coarse limestone gravel is in a poorer state of preservation than in other units. Gravel-sized clasts frequently exhibit dissolution cavities with rounded edges and dusty clay coatings. Components include angular bone fragments, both burnt and unburnt, and calcitic wood ash likely resulting from a reworked combustion feature in this unit.

4.3.3.3. S.U. III. This unit, which is composed of a thin cemented carbonate crust yielding very few archaeological remains, was represented in a single thin section, characterised by MF type 1. Components include bone fragments and rare faecal spherulites.

4.3.3.4. S.U. IVa-g. Subunit IVa is captured in two thin section samples and is predominantly characterised by the massive microstructure exhibited by MF type 4a, but also containing MF type 1a and MF type 2. The coarse mineral fraction generally occurs as subrounded to rounded and frequently fissured. Components include ash and frequent bone fragments.

Subunit IVb is composed of MF type 1b and MF type 3 with a crumb/granular to vughy microstructure. The calcitic matrix within this subunit shows slight dissolution and a porosity with a horizontal arrangement, indicative of cryoturbation. This subunit also contains a lower proportion of gravel relative to the other subunits within S.U IV. The medium and coarse gravel in subunit IVb is also more notably angular, regularly occurring with a lenticular or platy morphology, typical of frost affected sediments. Impregnation of iron oxides is also frequent and occurs both in the matrix and as fine silt sized nodules. The components are very similar to IVa.

Subunit IVc, which is a roof collapse deposit composed of boulders and large angular cobbles, due to the absence of fine

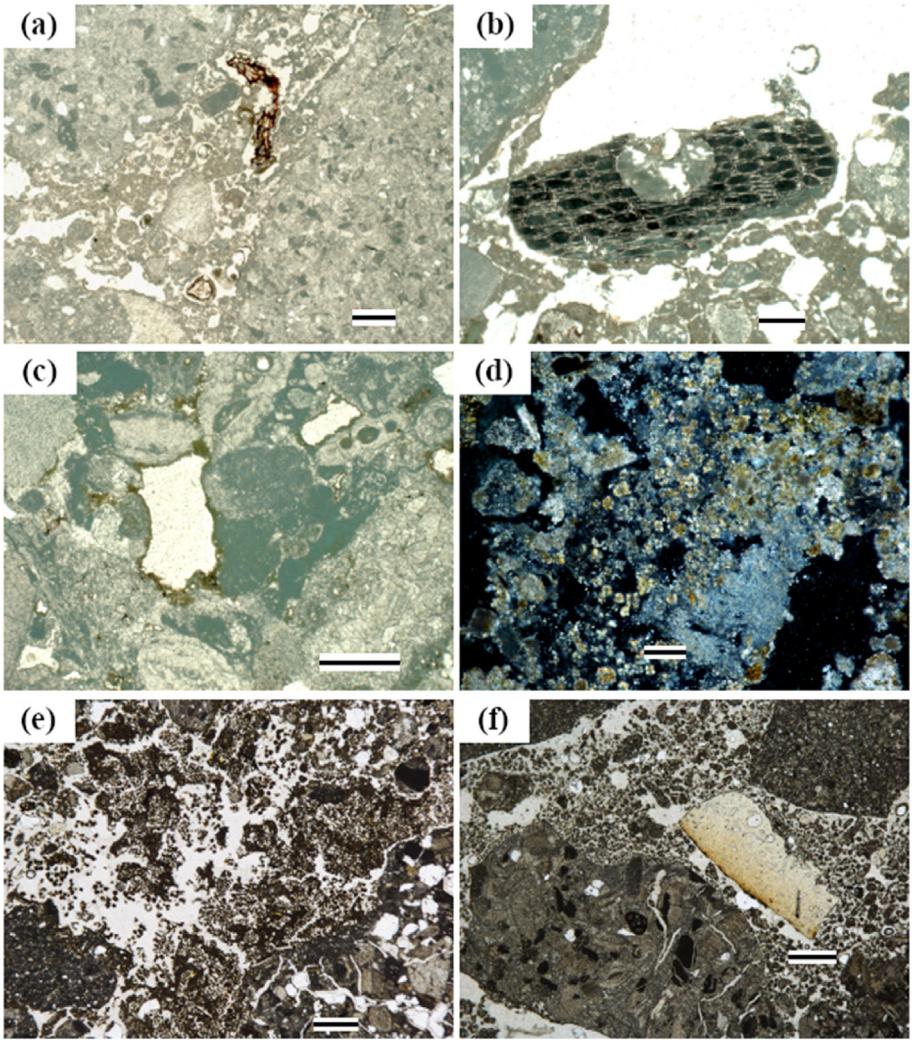

Fig. 9. Micromorphological components and features observed at Abric del Pastor (a) Fresh organic vegetal matter associated with root bioturbation (PPL, S.U. IVa, scale 500 μm) (b) Fragment of carbonised vegetal matter (PPL, S.U. II, scale 500 μm) (c) Dissolution well with fine dusty clay coating in limestone clast (PPL, S.U. II, scale 500 μm) (d) Faecal spherulites associated with reworked ashy aggregate (XPL, S.U. VI, 100 μm) (e) Bioturbated matrix with soil fauna excrements (PPL, S.U. IVd, 1000 μm) (f) Burnt bone in loose sandy sediment with crumb to granular microstructure, note the fissured clast (PPL, S.U. IVd, scale 1000 μm).

material has not been included in the micromorphological study.

Subunit IVd is characterised microscopically by MF type 1a and MF type 3, with a crumb/granular to spongy microstructure. A slightly higher proportion of gravel is recorded in this subunit relative to the other subunits within S.U IV. Again, clasts with a platy morphology are frequent. Dusty clay cappings and fissuring of clasts may be further evidence of mild cryoturbation. Components are similar to IVa and IVb but occur in higher abundances.

Subunits IVe and IVf are represented in two thin sections, characterised by MF type 1 and MF type 1a, with an open crumb to granular microstructure. Well-rounded clasts, fissuring and clay cappings are frequent. Similar to the other subunits in S.U. IV, components include bone fragments, reworked ash and charcoal.

Subunit IVg is represented in three thin sections and is characterised by MF type 1 with an open crumb to granular microstructure. A higher proportion of gravel occurs in this subunit relative to the overlying subunits. Fe and Mn impregnation features were also identified. Anthropogenic components, such as ash or charcoal, are greatly reduced in quantity within this subunit.

4.3.3.5. S.U. V. This unit is represented in a single thin section characterised by MF type 1. Lithologically this unit is very similar to S.U IVa with a calcitic matrix and an open crumb to granular microstructure. The matrix is slightly permeated by iron oxides and clay coatings. Components include rare charcoal and bone fragments.

4.3.3.6. S.U. VI. This unit is characterised by MF type 1 with an open crumb to granular microstructure which is locally compacted. Corroded and fissured clasts in this unit are similar to those recorded in S.U II. Anthropogenic components include burnt bone, charcoal, calcitic wood ash and fat derived char. These occur in much greater abundances than other units. Faecal spherulites are recorded here mixed with reworked combustion residues. Dusty clay coatings and infillings are common. Needle fibre calcite is also recorded here in-filling the interstitial pore space.

4.4. Anthracological remains

Anthracological data from Abric del Pastor has been partially published in previous works. Here, anthracological data from S.U. IVc, IVd1, IVd2 (Vidal-Matutano et al., 2015) and S.U. IVd3 (Vidal-

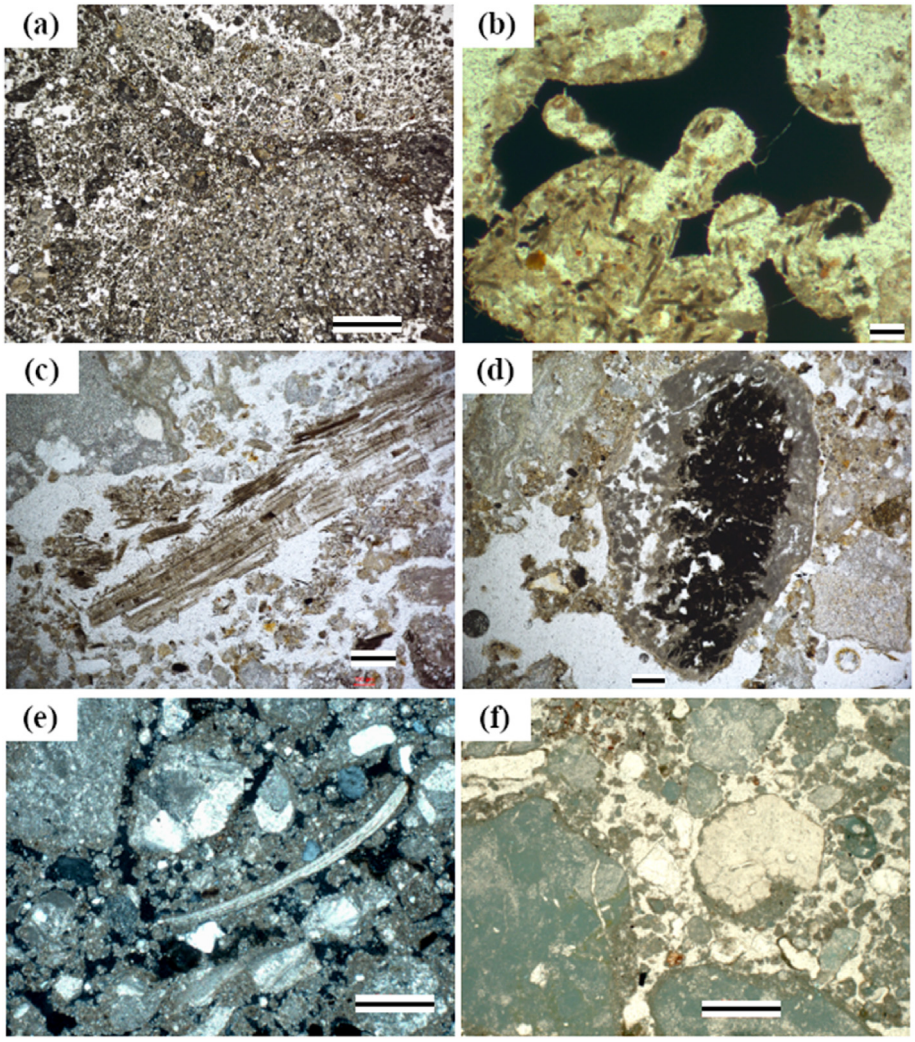

Fig. 10. Micromorphological components and features observed at Abric del Pastor (a) Soil crust (PPL, S.U. IVd, scale 1000 μm) (b) Fragment of fat derived char (PPL, S.U. VI, scale 1000 μm) (c) Partially carbonised and ashed plant material (PPL, S.U. VI, scale 100 μm) (d) Reworked ashy aggregate (XPL, S.U. VI, scale 1000 μm) (e) Fragment of terrestrial snail shell (XPL, S.U. I, scale 500 μm) (f) Massive coprolite (PPL, S.U. I, scale 500 μm).

Matutano et al., 2017) is presented together with new anthracological data from S.U IVd4 and S.U. IVd5 (Table 3). The scattered charcoal assemblages analysed from units IVc and IVd (IVd1-5) at Abric del Pastor include a total of 957 charcoal fragments and at least 19 taxa have been identified. Despite the small size of most of the wood charcoal remains (1–2 mm) and its scarcity in some units, a high variety of taxa indicating the presence of several plant formations in the surroundings can be inferred. Charcoal data from IVd2 and IVd3 has been unified here as data for each unit was not statistically representative (<100 remains).

The most representative taxa throughout S.U IV from Abric del Pastor is *Juniperus* sp. (juniper) together with xeric taxa (Euphorbiaceae, *Ephedra* sp., Cistaceae) (Fig. 11). This overall pattern is seen throughout S.U. IVd and IVc (values of 36–58%). Values from *Pinus nigra-sylvestris* (black-scots pine) suggest a clear trend decreasing from 29% (S.U. IVd5) to 1% (S.U. IVc). In addition to this, Mediterranean mixed forest taxa including evergreen and deciduous *Quercus* (oaks), *Pistacia* sp. (terebinth), *Rosa* sp. (rose), *Prunus* sp. or Maloideae (Rosaceae family) are abundant throughout IVd4 - IVc (38–49%). Notably lower proportions of these taxa are, however, recorded in IVd5 (12%). Finally, riverine taxa such as Ulmaceae (the elm family), *Salix-Populus* (willow-poplar) and *Fraxinus* sp. (ash) are present in small amounts (values < 7%). We infer two distinct anthracological phases from the analysed remains (AP-1 and AP-2). Phasing is a preliminary assessment of the data which relies on grouping analytical units to infer periods of distinct environmental conditions.

4.5. Microvertebrate study (S.U.IVd)

The small vertebrate assemblage from the S.U. IVd contains 295 dental and bone remains that correspond to 33 individuals. The faunal list of this unit contains 3 rodents (*Microtus cabrerae*, *Eliomys quercinus* and *Apodemus sylvaticus*), 1 insectivore (*Crocidura* gr. *russula-gueldenstaedtii*), 1 anuran (*Pelodytes* sp.), 2 lizards (cf. *Timon lepidus* s. l. and cf. *Podarcis* sp.) and 3 snakes (Colubridae indet., *Coronella girondica* and Viperidaea indet.) (supplementary figure SF 2).

The studied assemblage is characterised by the dominance of *Apodemus sylvaticus* (MNI = 15), followed by cf. *Podarcis* sp. (MNI = 8), *Eliomys quercinus* (MNI = 3) and *Microtus cabrerae*, *Crocidura* gr. *russula-gueldenstaedtii*, *Pelodytes* sp., cf. *Timon Lepidus* s. l., Colubridae indet., *Coronella girondica* and Viperidae indet. (MNI = 1) (Table 4).

Table 3
New charcoal data from Abric del Pastor (IVd 4 and IVd5), presented here with S.U. IVc, IVd1, IVd2 (Vidal-Matutano et al., 2015) and S.U. IVd3 (Vidal-Matutano et al., 2017). Note that data from IVd2 and IVd3 are joined here because the total number of wood charcoal fragments for each unit is not statistically representative.

Stratigraphic Unit	IV c		IV d 1		IV d 2	IV d 3		IV d 4		IV d 5	
Taxa	n	%	n	%	n	n	%	n	%	n	%
Cistaceae	1	0.37	1	0.58	*	*	*	*	*	*	*
Ephedra sp.	5	1.84	*	*	*	*	*	*	*	*	*
Euphorbiaceae	4	1.47	1	0.58	*	*	*	*	*	*	*
Fabaceae	5	1.84	8	4.62	4	7	7.78	6	3.13	*	*
Fraxinus sp.	1	0.37	*	*	*	5	5.56			*	*
Juniperus sp.	145	53.31	93	53.76	28	28	31.11	65	33.85	90	54.55
Labiatae	7	2.57	*	*	*	*	*	1	0.52	*	*
Maloideae	3	1.10	13	7.51	*	*	*	1	0.52	*	*
Monocotyledoneae tp. Poaceae	1	0.37	*	*	*	*	*	*	*	*	*
Pinus nigra-sylvestris	4	1.47	8	4.62	3	8	8.89	38	19.79	44	26.67
Pistacia sp.	39	14.34	20	11.56	23	8	25.56	5	2.60	3	1.82
Prunus sp.	*	*	*	*	*	*	*	2	1.04	*	*
Quercus sp.	10	3.68	11	6.36	6	9	10.00	41	21.35	12	7.27
Quercus sp. deciduous	*	*	*	*	*	*	*	5	2.60	*	*
Quercus sp. evergreen	41	15.07	12	6.94	1	14	15.56	14	7.29	5	3.03
Rhamnus-Phillyrea	*	*	*	*	*	*	*	7	3.65	*	*
Rosa sp.	*	*	2	1.16	*	*	*	*	*	*	*
Salix-Populus	2	0.74	2	1.16	*	7	7.78	3	1.56	9	5.45
Taxus baccata	*	*	2	1.16	*	4	4.44	4	2.08	1	0.61
Ulmaceae	4	1.47	*	*	*	*	*	*	*	1	0.61
Total fragments	**272**	100	**173**	100	**65**	**90**	100	**192**	100	**165**	100
Total taxa	**14**		**11**		**6**	**9**		**13**		**7**	

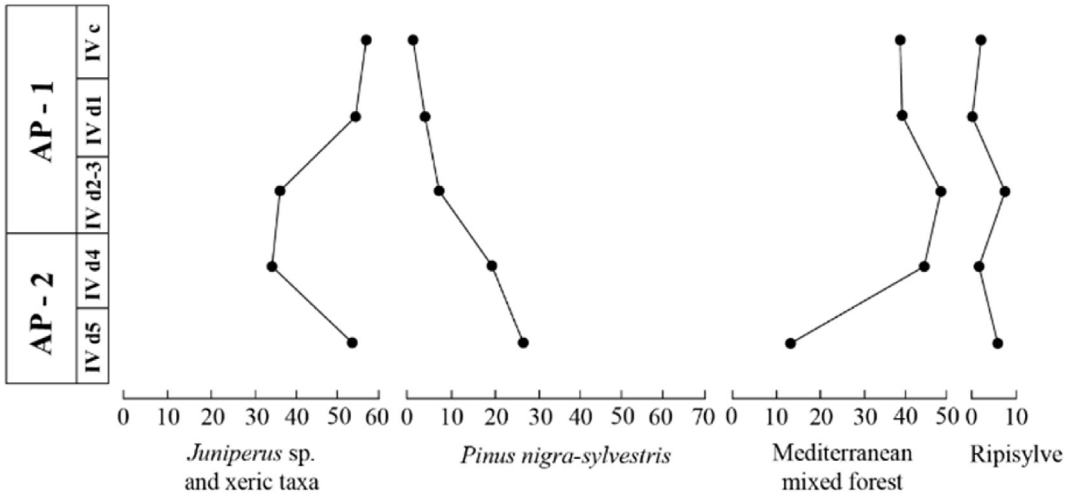

Fig. 11. Anthracological data (main plant formations) from Abric del Pastor (IVc – IVd5).

Palaeoecological reconstruction using the MER method indicates a MAT slightly lower than present conditions (−1.48 °C) (Table 5). Other climatic parameters such as MTC (−1.05 °C) and MTW (−0.78 °C) point to a cooler climate with precipitation values ranging from 411 mm to 837 mm (MAP 624.13 mm). As only generalist species have been included in the reconstruction, the entire range of possible values should be considered.

4.6. Macrofaunal study (S.U. IVd)

A total of 476 faunal remains has been analysed for this study, 46% of which have been taxonomically determined. Artiodactyls, composed at species level by *Bos primigenius*, *Capra pyrenaica* and *Cervus elaphus*, are the most frequent group among ungulates (73 NR), while perissodactyls are represented only by *Equus ferus* (1 NR). Testudines are the taxonomic category with the greatest number of identified remains in the assemblage (129 NR), all attributed to *Testudo hermanni*. Few remains of rabbit (*Oryctolagus cuniculus*, 8 NR), undetermined birds (2 NR) and small carnivore (1 NR) have also been recorded. The remaining 54% of the assemblage has not been determined taxonomically but can be associated with a weight size category. Medium size is the most abundant category (76 NR), followed by mall (23 NR), very small (5 NR) and large (2). A total of 142 NR could not be determined (Table 6).

The fragmentation rate is high, with most of the remains measuring <2 cm in length. Diagenetic alterations were observed throughout the assemblage, with a total of 574 surface damage features identified: concretions (42%), manganese oxide staining (29%), root-marks (15%), corrosion (8%), weathering (5%) and gnaw marks (1%). The skeletal material contains a high quantity of cranial remains, mainly in the form of isolated teeth of *Bos primigenius* and *Capra pyrenaica*, while long bone fragments occur more frequently among *Cervus elaphus*. In the case of tortoise, backplate fragments and plastron are relatively abundant. Conservation analysis by bone

Table 4
Number of Identified Specimens (NISP), Minimum Number of Individuals (MNI) and percentage of representation (%) of small vertebrates from the Unit IVd from Abric del Pastor. Distribution by habitat: OWo: Open Woodland; Wo: Woodland/Edge-woodland, OD: Open Dry, OH: Open Humid, Wa: Water and R: Rocky. Those species in open nomenclature indicate that these taxa could not be classified to the specific habitat level (dashes).

Taxon	NISP	NMI	%	OD	OH	OWo	Wo	R	W
Microtus cabrerae	6	1	3.03	0	0.50	0.50	0.00	0.00	0.00
Eliomys quercinus	9	3	9.09	0	0.10	0.40	0.30	0.20	0.00
Apodemus sylvaticus	125	15	45.45	0	0.25	0.50	0.25	0.00	0.00
Crocidura russula-gueldenstaedtii	2	1	3.03	0.40	0.10	0.40	0.10	0.00	0.00
Pelodytes sp.	1	1	3.03	0.33	0.16	0.25	0.08	0.16	0.00
Lacertidae indet.	21	–	–	–	–	–	–	–	–
cf. *Timon lepidus* s.l.	5	1	3.03	–	–	–	–	–	–
cf. *Podarcis* sp.	16	8	24.24	–	–	–	–	–	–
Serpentes indet.	2	–	–	–	–	–	–	–	–
Colubridae indet.	5	1	3.03	–	–	–	–	–	–
Coronella girondica	7	1	3.03	0.25	0.05	0.35	0.20	0.15	0.00
Viperidae indet.	1	1	3.03	–	–	–	–	–	–
Total	**200**	**33**	**100**	**4**	**22**	**47**	**23**	**4**	**0**

Table 5
Values of climatic parameters in the region around Alcoy today based on Hijmans et al. (2005) and those obtained through the MER method from the micro-vertebrate assemblage of S.U. IVd. SD = standard deviation; Max. = maximum; Min. = minimum; Δ = difference with present day conditions. MAT = mean annual temperature; MTC = minimum temperature of the coldest month; MTW = maximum temperature of the warmest month; MAP = mean annual precipitation; PWM = precipitation of wettest month; PDM = precipitation of driest month.

	Mean	SD	Max.	Min.	Δ	Alcoy
MAT	12.22	2.85	18.3	−0.2	−1.48	13.7
MTC	0.65	2.88	8.4	−11.4	−1.05	1.7
MTW	27.72	3.47	35.9	11.8	−0.78	28.5
MAP	624.13	212.92	1586	220	81.83	542.3
PWM	77.72	26.25	251	32	3.42	74.3
PDM	23.02	16.09	101.0	0.0	7.82	15.2

Table 6
Faunal remains from S.U. IVd.

Taxa	NISP/NR	MNE	MNI
Artiodactyla	8	7	–
Bos primigenius	2	2	1
Caprinae	16	16	2
Capra pyrenaica	28	23	2
Cervidae	5	2	1
Cervus elaphus	14	9	3
Equus ferus	1	1	1
Oryctolagus cuniculus	8	8	2
Testudinidae	5	5	1
Testudo hermanni	100	78	4
Testudo sp.	29	29	2
Small carnivore	1	1	1
Birds	2	2	1
Total NISP	**219**	**183**	**21**
Large size	2	–	–
Medium size	76	–	–
Small size	32	–	–
Very small size	5	–	–
Undetermined	142	–	–
Total NR	**257**	**-**	**-**

density shows a statistically significant positive correlation ($p < 0.05$) in wild goat (0.66) and cervids (0.45), demonstrating an important bias in part of the assemblage. For this reason, utility indices were not applied.

A total of 184 old fractures (fresh and dry) have been identified. They are mainly present in the long bones of ungulates, in the medium-weight size category and to a minor extent in cranial and coxal fragments, scapulae ribs, and a small quantity of tortoise plates. A large proportion of fresh fractures can be clearly linked to anthropogenic activity. See supplementary material for additional taphonomic data and information on anthropogenic surface alterations.

Our bioclimatic component calculations (supplementary figure SF 4) suggest that the most probable biome for the Abric del Pastor Unit IVd faunal assemblage is Type IV (Mediterranean) (Table 7).

5. Discussion

Leaf waxes derived from terrestrial higher plants are the predominant source of long chain length *n*-alkanes (nC_{27}– nC_{35}) at Abric del Pastor. Although long chain homologues (nC_{27}– nC_{35}) derived from higher plants dominate through most of the sequence, sediment samples collected from S.U IVd and S.U. IVc yielded *n*-alkane distributions with proportionally increased concentrations of mid-chain length homologues (nC_{18} to C_{26}) which do not display a strong odd-over-even predominance. Although microbial degradation can alter the chain length distribution of *n*-alkanes (Brittingham et al., 2017), a more likely explanation here may be the incorporation of charred biomass related to anthropogenic combustion activities. Although care was taken during sampling to avoid thermally altered sediments, dispersed ash, charcoal and burned bone are recorded elsewhere in these units at the micro-stratigraphic scale. Furthermore, at least eight discreet combustion features have been recorded during the excavation of S.U. IVd, more than in any other unit (Mallol et al., 2019). Studies elsewhere have demonstrated the effects of thermal degradation on *n*-alkane preservation and distributions (Eckmeier and Wiesenberg, 2009; Wiesenberg et al., 2009; Diefendorf et al., 2015b; Wang et al., 2017; Jambrina-Enríquez et al., 2018). With increasing temperatures, there is a decrease in chain length and a modification of the carbon preference from odd to even homologues, lowering ACL and CPI values. The *n*-alkane distributions and observed co-variance of ACL and CPI in S.U. IVd and IVc could therefore be explained by the effects of anthropogenic fire.

$\delta^{13}C_{wax}$ values are within the expected limits for a predominant contribution from C3 plants (Ficken et al., 1998). Through the entire sequence, there is a range of up to 5.6‰ (nC_{29}) and 6.7‰ (nC_{31}) for carbon isotope values, and up to 41‰ (nC_{29}) and 37‰ (nC_{31}) for hydrogen isotope values. $\delta^{13}C_{wax}$ decreases from −32.5‰ to −34.9‰ (nC_{29}) and −34.1‰ to −35.9‰ (nC_{31}) between the base and the uppermost part of S.U. IVd, while $\delta^{2}H_{wax}$ decreases from −136‰ to −152‰ (nC_{29}), and from −149‰ to −159‰ (nC_{31}). Although thermal alteration may have contributed to the observed variability (Wiesenberg et al., 2009), notably in S.U. IVd and IVc, $\delta^{13}C_{wax}$ and $\delta^{2}H_{wax}$ values through the sequence are likely

Table 7
Climate restriction index (CRI), bioclimatic component (BC), annual average temperature (AAT) and precipitation index (AAP).

Species	I	II	II/III	III	IV	V	VI	VII	VIII	IX	Total
Capra hircus	0.000	0.000	0.000	0.000	1.000	0.000	0.000	0.000	0.000	0.000	1.000
Cervus elaphus	0.000	0.000	0.000	0.000	0.333	0.000	0.333	0.333	0.000	0.000	0.999
Bos frontalis	0.000	0.000	0.000	0.000	0.333	0.333	0.333	0.000	0.000	0.000	0.999
Equus onager	0.000	0.000	0.000	0.333	0.333	0.000	0.000	0.333	0.000	0.000	0.999
Vulpes vulpes	0.000	0.000	0.000	0.143	0.143	0.143	0.143	0.143	0.143	0.143	1.001
O. cuniculus	0.000	0.000	0.000	0.000	1.000	0.000	0.000	0.000	0.000	0.000	1.000
Testudo hermanni	0.000	0.000	0.000	0.000	0.500	0.500	0.000	0.000	0.000	0.000	1.000
P. pyrrhocorax	0.000	0.000	0.000	0.333	0.333	0.333	0.000	0.000	0.000	0.000	0.999
CRI	**0.000**	**0.000**	**0.000**	**0.809**	**3.975**	**1.309**	**0.809**	**0.809**	**0.143**	**0.143**	**7.997**
BC	**0.000**	**0.000**	**0.000**	**10.116**	**49.706**	**16.368**	**10.116**	**10.116**	**1.788**	**1.788**	**100**
AAT	**17.711**										
SD	**3.751**										
AAP	**268.349**										
SD	**558.709**										

influenced by numerous factors. Water availability, temperature changes and specific plant attributes can all affect fractionation of carbon isotopes by plants during CO_2 uptake and fixation (Δ_{leaf}) (Kaplan et al., 2002; Diefendorf and Freimuth, 2017). Diefendorf et al. (2010) have demonstrated that MAP is a strong predictor of Δ_{leaf}, although factors such as microclimate and ecosystem structure are also likely to influence $\delta^{13}C_{wax}$. Precipitation δ^2H, evapotranspiration and vegetation type are considered direct controls δ^2H_{wax} values, although other environmental and physiological variables can exert secondary controls (Sachse et al., 2006, 2009; 2012; Liu and Yang, 2008; Liu and An, 2018). Changes in moisture source (Z. Liu et al., 2008; Tipple et al., 2015) or fluctuations in the intensity of the North Atlantic Oscillation (NAO) could play a role in determining precipitation patterns and δ^2H values (Muñoz-Díaz and Rodrigo, 2004; Brittingham et al., 2019), explaining some of the variability observed through the sequence at Abric del Pastor. North Atlantic dynamics have been shown to play a significant role in the isotopic composition and variability of precipitation (Benetti et al., 2017). These effects have been recorded elsewhere in the Iberian Peninsula (Jambrina-Enríquez et al., 2017). A negative correlation between monthly precipitation amount and precipitation δ^2H recorded at GNIP (Global Network for Isotopes in Precipitation; IAEA/WMO, 2006) stations in Murcia and Valencia suggests that regional δ^2H_p values may be influenced to some extent by precipitation amount. Temperature is also likely to have been a significant factor, however, as this plays a role in governing soil water evaporation and leaf transpiration, which in turn affects the primary signal (Sachse et al., 2012; Kahmen et al., 2013; Wang et al., 2016). Water availability is an important control on $\delta^{13}C$ in C3 plants, which has also previously been shown in certain cases to positively correlate with MAP and relative humidity (RH) (Farquhar et al., 1989; Diefendorf et al., 2010; Garcin et al., 2014; Diefendorf and Freimuth, 2017). Co-varying trends between δ^2H_{wax} and $\delta^{13}C_{wax}$ through the sequence at Abric del Pastor could therefore be linked to the combined effects of changes in moisture source, precipitation amount and fluctuations in temperature and evaporative stress.

Evidence of generally cool conditions throughout the sequence are recorded at the microstratigraphic level by the occurrence of weakly lenticular and granular microstructures, in addition to features such as soil cappings, and frequent platy or fissured clasts characteristic of cyclical freeze-thaw processes (Vliet-Lanoë, 2010). The sequence is generally composed of laterally discontinuous sands and gravels derived from the collapse and disintegration of the limestone conglomerate which makes up the rock shelter. Faecal spherulites recorded in S.U. I may be linked to the presence of goats at the site in relatively recent times. In addition to input of fresh leaves from the modern trees and vegetation immediately adjacent to the site, this probably contributes to the elevated TOC values in S.U. I. Other sources may include the frequent occurrence of fresh root-derived OM which has been observed in several thin sections. This highlights the effects of active bioturbation, although, it should be noted that this does not uniformly affect entire the sequence, being more intense in the uppermost units (S.U. I - IVa). Good preservation of the calcitic matrix, sedimentary components and anthropogenic material throughout most of the sequence signal generally high rates of sedimentation. Indicators of slower sedimentation rates, increased surface exposure and the presence of moisture also occur, however, in the form of redoximorphic features and instances where it is evident that the calcitic matrix has been affected by dissolution processes. This is observed in S.U. IVd, for instance, and might partially explain the degree of thermal degradation affecting *n*-alkane distributions as slower sedimentary rates produce a palimpsest effect with the concentration and superimposition of materials related to successive combustion events (Bailey, 2007; Machado et al., 2015). The occurrence of textural contrasts and sharp contacts between depositional facies suggest sedimentary accretion at the site is dynamic and responsive to external processes, most likely linked to shifting environmental conditions.

Cool temperatures are also implied by the charcoal assemblage from S.U. IVc and IVd which shows a predominance of juniper (>50% in some subunits) relative to pine, coherent with the establishment of a cold climate during which heliophilous, drought-tolerant plants progressively developed, accompanied by a decrease in temperatures throughout the Iberian Peninsula (Sánchez-Goñi et al., 1999). Our reconstruction points to dry or semi-arid supramediterranean conditions (MAT of 8–13 °C, −4 °C and MAP of 200–600 mm, −80 mm), which is congruent with the observed δ^2H_{wax} and $\delta^{13}C_{wax}$ values if we accept that temperature and evaporative stress are the dominant controls. Indeed, juniper species show great resistance to changes in temperature and humidity, being physiologically adapted to stress tolerance with low demands in terms of soil (Costa et al., 2005). The homogenous anatomical structure of *Juniperus* does not allow for the discrimination of the species gathered, which could hypothetically include thermophilous species (*J. oxucedrus, J. phoenicea*) or cryophilous ones (*J. communis, J. thurifera, J. sabina*), whose present-day range covers from thermo-Mediterranean to supra-Mediterranean bioclimatic belts together with dry or semi-arid conditions (Costa et al., 2005). However, carpological data from El Salt, a Middle Palaeolithic site located 4 km away from Abric del Pastor, indicate the presence of *Juniperus sabina* (savin juniper) in the region (units VIII – Xa), at least during MIS 3 (Vidal-Matutano et al., 2017). This taxon is currently abundant in the supra-Mediterranean and oro-

Mediterranean bioclimatic belts, above 1100–1200 m a.s.l., occurring together with other species of the same genus (*J. communis, J. thurifera*) (Rivas-Martínez, 1987; Costa et al., 2005). The absence of thermophilous juniper at Abric del Pastor would be consistent with an anthracological assemblage reflecting a temperature range which is lower than present conditions. The appreciable percentage of mixed forest taxa in those units coinciding with decreasing values of juniper might be explained by the location of the rock shelter in a narrow ravine, where access to several plant formations is possible within a short distance (<1 km). The presence of these plant formations, with different ecological requirements to juniper, point to the existence of a local vegetation refugium, composed of several biotopes, facilitated by the orography of the narrow ravine.

The current spatial distribution of plant taxa recorded in S.U. IV has been obtained for the Iberian Peninsula, taking into account *Juniperus communis, Juniperus ocycedrus, Juniperus phoenicea, Juniperus thurifera, Juniperus sabina, Pinus nigra* subsp. *salzmanii, Pinus nigra* subsp. *Arnold, Taxus baccata, Pistacia terebinthus, Quercus ilex ballota* and *Quercus faginea*. This is presented here alongside the distribution of the microfaunal species recorded in S.U. IVd (Fig. 12). The Javalambre and Gúdar mountain ranges (Teruel) and the eastern Iberian mountain system show the highest proportions of overlapping plant taxa. This mountainous region (1000–1500 m a.s.l.) is located at the supramediterranean bioclimatic belt with a MAT of 8–10 °C and a MAP of 400–600 mm (Rivas-Martínez, 1987). Isolated locations are also highlighted in the Pyrenees and the Central and Betic mountain systems.

Our palaeoecological reconstruction based on the microfauna suggests a similar scenario, with generally cooler (MAT -1.48 °C) and possibly drier (411 mm–837 mm) conditions than present. The Habitat Weighting Method indicates a predominance of open woodland environments (47%) (supplementary figure SF 3), which includes woodland margins and forest patches with moderate ground cover, evidenced by the abundance of *Apodemus sylvaticus*. This species is ubiquitous throughout Spain, normally occupying areas with a good shrub or tree cover (Palomo et al., 2007). Woodlands and Open Humid habitats are next most-commonly represented habitat types in S.U. IVd, although values are only approximately half those obtained for Open Woodland habitats, at 23% and 22% respectively. Species linked to rocky environments such as *Eliomys quercinus, Pelodytes* sp., *Coronella girondica* and Viperidae indet. are probably explained by the topographic context of the site, near a cliff. The presence of temporary water bodies is indicated by the remains of *Pelodytes* sp., despite appearing in lower proportions. The probable agent responsible for the accumulation of the assemblage, *Bubo bubo*, is a nocturnal raptor widespread throughout Europe and Asia (see supplementary material). This species depends on a wide range of prey and its associated prey assemblages are taxonomically diverse with a high degree of equitability.

The macrofaunal assemblage from S.U. IVd is characteristic of Mediterranean conditions. Climatic reconstruction based on the CRI model yielded an AAP value of 268 mm, which is consistent with ranges obtained from other proxies. Variation in the proposed temperature values between the different datasets probably reflect the disparate depositional agents responsible for their accumulation and the differing spatial resolutions of the proxies. The taxonomic composition of the assemblage is potentially congruent with either an MIS 5 setting, or a phase of climatic amelioration during MIS 4. As such, the frequent occurrence of Mediterranean tortoise (*Testudo hermanni*) in S.U. IVd is notable. In Pleistocene chronologies, there are few archaeological deposits in the Mediterranean area where *Testudo hermanni* is present during MIS 4, limited to Cova Dalt del Tossal de la Font (MIS5d-4) and Abric del Pastor (Morales and Sanchis, 2009; Sanchis et al., 2015; Mallol et al., 2019). In fact, a recent review of Neanderthal consumption of *Testudo hermanni* in the Iberian Peninsula by Nabais and Zilhão (2019) suggests that the species may have almost completely disappeared from the peninsula at the onset of MIS 4 as a result of over-exploitation. It's presence at Abric del Pastor is in agreement with the anthracological data which suggests that the ravine where the site is located probably acted as a vegetation refugium,

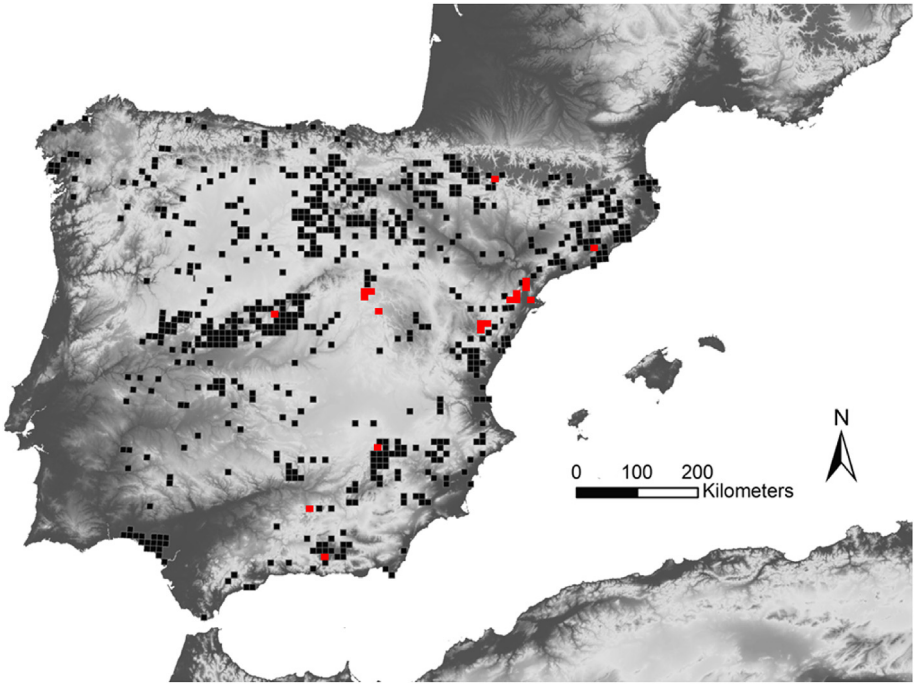

Fig. 12. 10 × 10 UTM squares obtained overlapping the distribution areas of the main plant (red squares) and small mammal, reptile and amphibian (black squares) species analysed in this study. (For interpretation of the references to colour in this figure legend, the reader is referred to the Web version of this article.)

providing sufficient tree and shrub cover for this species to thrive, as well as an abundant and diverse source of woody biomass which could be exploited as fuel by Neanderthal groups.

The resolution of the current chronological framework at Abric del Pastor limits the direct comparisons which can be drawn between our sequence and other regional palaeoclimate records. Nevertheless, our most complete dataset comes from S.U. IVd, which corresponds with an OSL date of 63 kya ±5000 (1σ), implying an MIS 4 or possible late MIS 5 setting. During the period in question, evidence from the upper Tagus Basin suggests the accumulation of significant loess deposits are linked to cool and dry conditions through MIS 4, but perhaps began accumulating as early as late MIS 5 (Wolf et al., 2018). This might point to the development of adverse environmental conditions in the Iberian interior, with decreasing vegetation cover limiting the availability of important resources. In such a scenario, peripheral regions along the Iberian coastline may have been more climatically favourable for Neanderthal groups. Pollen records from Area Longa (Galicia) in the north-west of the peninsula record a stadial vegetation with grassland and heathland through the earliest stages of MIS 4 (Gómez-Orellana et al., 2007; Fletcher et al., 2010), while palynological records from Abric Romaní, in the north-east, record a predominance of steppe vegetation (*Artemisia*) characteristic of generally dry and cold conditions, interspersed by rapid episodic shifts in vegetation structure which led to an increase in grasses (Poaceae) followed by a decline in pines and deciduous oaks (*Quercus*). The presence of *Betula* with *Corylus*, *Viburnum* and Mediterranean taxa, suggest that localised glacial refugia persisted during MIS 4 (Burjachs and Julià, 1994; Biltekin et al., 2019). This is in keeping with the data presented here from Abric del Pastor and taken together could predict similar conditions for MIS 4 throughout the Eastern Iberian Peninsula, pointing to a mosaic scenario with different biotopes shaped by local geographic factors.

6. Concluding remarks

Drawing on multiple lines of evidence, we have investigated climatic variability through the sequence at Abric del Pastor. Our data points to a generally cold but variable climate through the Plesitocene part of the sequence, as evidenced by the persistent presence of cryoturbation features in our micromorphological samples. *n*-Alkane distributions and co-varying CPI and ACL values in S.U. IVc and IVd reflect degradation linked to the probable incorporation of charred biomass associated with anthropogenic burning events. This is supported by the archaeological evidence at the macroscopic scale where eight combustion features are recorded in S.U. IVd, as well as at the microstratigraphic scale where combustion residues are linked to microfacies which show signs of slower sedimentary rates. Fluctuations in δ^2H_{wax} and $\delta^{13}C_{wax}$ through the sequence can be explained as the combined effects of moisture source changes, regional precipitation amount and changes in atmospheric temperatures. This is consistent with our anthracological analysis of S.U. IVc and IVd which indicates a prevalence of dry to semi-arid supramediterranean conditions (MAT -4 °C and MAP of 200–600 mm, −80 mm) and our reconstruction based on the small-mammal assemblage (MAT -1.48 °C, MAP 411 mm–837 mm). At this part of the sequence, which corresponds with an OSL date of 63 kya (±5000 1σ), we propose a scenario where open dry woodland formations extended throughout the upper reaches of the valley, while Mediterranean mixed forest taxa and riverine species survived within the Barranc del Cinc ravine, a vegetation refugium providing adequate tree cover and ground shrubs to support species such as *Testudo hermanni,* which were exploited for subsistence by Neanderthal groups. The ravine also provided an abundant fuel source in the form of woody biomass. The occupation of the rock shelter may have formed part of a broad subsistence and mobility strategy focused on intra-mountainous valleys or ravines, like the Barranc del Cinc, which are zones of ecological resilience and biodiversity that provide opportunities for the construction of crucial econiches. Finally, our results demonstrate the utility of a coupled biomolecular and geoarchaeological approach, however, encourage caution for future studies in archaeological contexts where microscopic residues, related to anthropogenic fire for instance, can potentially influence the molecular or isotopic signal. In such cases, soil micromorphology is a powerful tool for determining the extent of anthropogenic impact on sediments and establishing vital constraints for the interpretation of biomolecular data.

CRediT authorship contribution statement

Rory Connolly: Conceptualization, Investigation, Formal analysis, Writing - original draft. **Margarita Jambrina-Enríquez:** Validation, Writing - review & editing. **Antonio V. Herrera-Herrera:** Validation, Writing - review & editing. **Paloma Vidal-Matutano:** Investigation, Formal analysis, Writing - original draft. **Ana Fagoaga:** Investigation, Formal analysis, Writing - original draft. **Rafael Marquina-Blasco:** Investigation, Formal analysis, Writing - original draft. **María Dolores Marin-Monfort:** Investigation, Formal analysis, Writing - original draft. **Francisco Javier Ruiz-Sánchez:** Investigation, Formal analysis, Writing - original draft. **César Laplana:** Investigation, Formal analysis, Writing - original draft. **Salvador Bailon:** Investigation, Formal analysis, Writing - original draft. **Leopoldo Pérez:** Investigation, Formal analysis, Writing - original draft. **Lucia Leierer:** Writing - review & editing. **Cristo M. Hernández:** Writing - review & editing. **Bertila Galván:** Writing - review & editing. **Carolina Mallol:** Conceptualization, Supervision, Writing - review & editing, Project administration, Resources, Funding acquisition.

Acknowledgements

This research was supported by the ERC Consolidator Grant project PALEOCHAR — 648871. Excavations at Abric del Pastor are funded by Spanish Ministry of Science, Innovation and Universities Project HAR2015-68321-P and the Government of Valencia Cultural Heritage Department. The authors would like to thank Caterina Rodríguez de Vera, Santiago Sossa Ríos and Glenn Lambrecht for their work and assistance at AMBI lab, as well as all of those, past and present, who have been involved in carrying out the excavation fieldwork at Abric del Pastor.

Appendix A. Supplementary data

Supplementary data to this article can be found online at https://doi.org/10.1016/j.quascirev.2019.106023.

References

AHE, 2016. SIARE (Servidor de Información de Anfibios y Reptiles de España). Asociación Herpetológica Española. http://siare.herpetologica.es/bdh. (Accessed November 2018).

Alcaraz-Castaño, M., Alcolea-González, J., Kehl, M., Albert, R.-M., Baena-Preysler, J., de Balbín-Behrmann, R., Cuartero, F., Cuenca-Bescós, G., Jiménez-Barredo, F., López-Sáez, J.-A., Piqué, R., Rodríguez-Antón, D., Yravedra, J., Weniger, G.-C., 2017. A context for the last Neandertals of interior Iberia: los Casares cave revisited. PLoS One 12, e0180823.

Badal, E., 1992. L'anthracologie préhistorique: à propos de certains problèmes méthodologiques. In: Vernet, J.-L. (Ed.), Les charbons de bois, les anciens écosystèmes et le rôle de l'homme, Montpellier, vol. 139. Société botanique de France (Bulletin de la Société botanique de France, pp. 167–190.

Badal, E., Heinz, C., 1991. Méthodes utilisées en Anthracologie pour l'étude de sites préhistoriques. BAR International Series 573, 17–47.
Bailey, G., 2007. Time perspectives, palimpsests and the archaeology of time. J. Anthropol. Archaeol. 26, 198–223.
Bailon, S., 1991. Amphibiens et reptiles du Pliocene et du Quaternaire de France et d'Espagne: mise en place et evolution des faunes. Ph.D. Thesis. Universite de Paris VII (Unpublished).
Bailon, S., 1999. Différenciation ostéologique des anoures (Amphibia, Anura) de France. Antibes. In: Desse, J., DesseBerset, N. (Eds.), Fiches d'Ostéologie Animale Pour l'Archéologie, 1–42. Centre de Recherches Archéologiques du CNRS, APDCA, série C, varia.
Barahona, F., 1996. Osteología craneal de lacértidos de la Península Ibérica e Islas Canarias: análisis sistemático filogenético. Ph.D. Thesis,. Universidad Autónoma de Madrid (Unpublished).
Barahona, F., Barbadillo, L.J., 1997. Identification of some Iberian lacertids using skull characters. Rev. Espanola Herpetol. 11, 47–62.
Benetti, M., Steen-Larsen, H.C., Reverdin, G., Sveinbjörnsdóttir, Á.E., Aloisi, G., Berkelhammer, M.B., Bourlès, B., Bourras, D., de Coetlogon, G., Cosgrove, A., Faber, A.-K., Grelet, J., Hansen, S.B., Johnson, R., Legoff, H., Martin, N., Peters, A.J., Popp, T.J., Reynaud, T., Winther, M., 2017. Stable isotopes in the atmospheric marine boundary layer water vapour over the Atlantic Ocean, 2012–2015. Scientific Data 4, 160128.
Bi, X., Sheng, G., Liu, X., Li, C., Fu, J., 2005. Molecular and carbon and hydrogen isotopic composition of n-alkanes in plant leaf waxes. Org. Geochem. 36, 1405–1417.
Biltekin, D., Burjachs, F., Vallverdú, J., Sharp, W.D., Mertz-Kraus, R., Gema Chacón, M., Saladié, P., Bischoff, J.L., Carbonell, E., 2019. Vegetation and climate record from abric Romaní (capellades, northeast iberia) during the upper Pleistocene (MIS 5d–3). Quat. Sci. Rev. 220, 154–164.
Blain, H.A., 2009. Contribution de la paléoherpétofaune (Amphibia & Squamata) à la connaissance de lévolution du climat et du paysage du Pliocène supérieur au Pléistocène moyen d'Espagne, vol. 16. Treballs del Museu de Geologia de Barcelona, pp. 39–170.
Blain, H.A., Bailon, S., Cuenca-Bescós, G., Arsuaga, J.L., Bermúdez de Castro, J.M., Carbonell, E., 2009. Long-term climate record inferred from Early-Middle Pleistocene amphibian and squamate reptile assemblages at the Gran Dolina cave, Atapuerca, Spain. J. Hum. Evol. 56, 55–65. https://doi.org/10.1016/j.jhevol.2008.08.020.
Blain, H.A., Gleed-Owen, C.P., López-García, J.M., Carrión, J.S., Jennings, R., Finlayson, G., Finlayson, C., Giles-Pacheco, F., 2013. Climatic conditions for the last Neanderthals: herpetofaunal record of gorham's cave, Gibraltar. J. Hum. Evol. 64, 289–299.
Blain, H.A., Laplana, C., Sevilla, P., Arsuaga, J.L., Baquedano, E., Pérez-González, A., 2014. MIS 5/4 transition in a mountain environment: herpetofaunal assemblages from Cueva del Camino, central Spain. Boreas 43, 107–120.
Blain, H.-A., Lozano-Fernández, I., Agustí, J., Bailon, S., Menéndez, L.G., Espígares, P.O.M., Ros-Montoya, S., Jiménez, J.M.A., Toro-Moyano, I., Martínez-Navarro, B., Sala, R., 2016. Redefining upon the climatic background of the early Pleistocene hominid settlement in western Europe: barranco leon and fuente nueva-3 (Guadix-Baza basin, SE Spain). Quat. Sci. Rev. 144, 132–144. https://doi.org/10.1016/j.quascirev.2016.05.02.
Bray, E.E., Evans, E., 1961. Distribution of n -paraffins as a clue to recognition of source beds. Geochem. Cosmochim. Acta 22, 2–15.
Brittingham, A., Hren, M.T., Hartman, G., 2017. Microbial alteration of the hydrogen and carbon isotopic composition of n-alkanes in sediments. Org. Geochem. 107, 1–8.
Brittingham, A., Petrosyan, Z., Hepburn, J.C., Richards, M.P., Hren, M.T., Hartman, G., 2019. Influence of the north atlantic oscillation on δD and δ18O in meteoric water in the Armenian highland. J. Hydrol 575, 513–522.
Bunn, H.T., 1986. Patterns of skeletal representation and hominid subsistence activities at Olduvai Gorge, Tanzania, and Koobi Fora, Kenya. J. Hum. Evol. 15, 673–690.
Burjachs, F., Julià, R., 1994. Abrupt climatic changes during the last glaciation based on pollen analysis of the abric Romani, catalonia, Spain. Quat. Res. 42, 308–315.
Bush, R.T., McInerney, F.A., 2013. Leaf wax n-alkane distributions in and across modern plants: implications for paleoecology and chemotaxonomy. Geochem. Cosmochim. Acta 117, 161–179.
Chabal, L., 1997. Forêts et sociétés en Languedoc (Néolithique final, Antiquité tardive) : l'anthracologie, méthode et paléoécologie. Éditions de la Maison des sciences de l'homme, Paris.
Chapman, M.R., Shackleton, N.J., 1999. Global ice-volume fluctuations, North Atlantic ice-rafting events, and deep-ocean circulation changes between 130 and 70 ka. Geology 27, 795–798.
Collins, J.A., Schefuß, E., Mulitza, S., Prange, M., Werner, M., Tharammal, T., Paul, A., Wefer, G., 2013. Estimating the hydrogen isotopic composition of past precipitation using leaf-waxes from western Africa. Quat. Sci. Rev. 65, 88–101.
Collins, J.A., Carr, A.S., Schefuß, E., Boom, A., Sealy, J., 2017. Investigation of organic matter and biomarkers from diepkloof rock shelter, South Africa: insights into Middle stone age site usage and palaeoclimate. J. Archaeol. Sci. 85, 51–65.
Costa, M., Morla, C., Sainz, H., 2005. Los Bosques Ibéricos: Una Interpretación Geobotánica. Editorial Planeta, Barcelona.
Courty, M.A., 2001. Microfacies analysis assisting archaeological stratigraphy. In: Goldberg, P., Holliday, V.T., Reid Ferring, C. (Eds.), Earth Sciences and Archaeology, 205–239. Springer US.
Courty, M.A., Vallverdu, J., 2001. The microstratigraphic record of abrupt climate changes in cave sediments of the Western Mediterranean. Geoarchaeology 16, 467–499.
Cranwell, P.A., Eglinton, G., Robinson, N., 1987. Lipids of aquatic organisms as potential contributors to lacustrine sediments—II. Org. Geochem. 11, 513–527.
Daams, R., 1981. The Dental Pattern of the Dormice Dryomys, Myomimus, Microdyromys and Peridyromys, vol. 3. Utrecht Micropaleontological Bulletins. Special Publications, pp. 1–115.
Dansgaard, W., 1964. Stable isotopes in precipitation. Tellus 16, 436–468.
Daura, J., Sanz, M., Julià, R., García-Fernández, D., Fornós, J.J., Vaquero, M., Allué, E., López-García, J.M., Blain, H.A., Ortiz, J.E., Torres, T., Albert, R.M., Rodríguez-Cintas, À., Sánchez-Marco, A., Cerdeño, E., Skinner, A.R., Asmeron, Y., Polyak, V.J., Garcés, M., Arnold, L.J., Demuro, M., Pike, A.W.G., Euba, I., Rodríguez, R.F., Yagüe, A.S., Villaescusa, L., Gómez, S., Rubio, A., Pedro, M., Fullola, J.M., Zilhão, J., 2015. Cova del Rinoceront (Castelldefels, Barcelona): a terrestrial record for the Last Interglacial period (MIS 5) in the Mediterranean coast of the Iberian Peninsula. Quat. Sci. Rev. 114, 203–227.
Daura, J., Sanz, M., Allué, E., Vaquero, M., López-García, J.M., Sánchez-Marco, A., Domènech, R., Martinell, J., Carrión, J.S., Ortiz, J.E., Torres, T., Arnold, L.J., Benson, A., Hoffmann, D.L., Skinner, A.R., Julià, R., 2017. Palaeoenvironments of the last Neanderthals in SW Europe (MIS 3): Cova del Coll Verdaguer (Barcelona, NE of Iberian Peninsula). Quat. Sci. Rev. 177, 34–56.
Diefendorf, A.F., Freimuth, E.J., 2017. Extracting the most from terrestrial plant-derived n-alkyl lipids and their carbon isotopes from the sedimentary record: a review. Org. Geochem. 103, 1–21.
Diefendorf, A.F., Mueller, K.E., Wing, S.L., Koch, P.L., Freeman, K.H., 2010. Global patterns in leaf 13C discrimination and implications for studies of past and future climate. Proc. Natl. Acad. Sci. U. S. A. 107, 5738–5743.
Diefendorf, A.F., Leslie, A.B., Wing, S.L., 2015a. Leaf wax composition and carbon isotopes vary among major conifer groups. Geochem. Cosmochim. Acta 170, 145–156.
Diefendorf, A.F., Sberna, D.T., Taylor, D.W., 2015b. Effect of thermal maturation on plant-derived terpenoids and leaf wax n-alkyl components. Org. Geochem. 89–90, 61–70.
d'Errico, F., Sánchez Goñi, M.F., 2003. Neandertal extinction and the millennial scale climatic variability of OIS 3. Quat. Sci. Rev. 22, 769–788.
Eckmeier, E., Wiesenberg, G.L.B., 2009. Short-chain n-alkanes (C16–20) in ancient soil are useful molecular markers for prehistoric biomass burning. J. Archaeol. Sci. 36, 1590–1596.
Eglinton, G., Hamilton, R.J., 1967. Leaf epicuticular waxes. Science 156, 1322–1335.
Eglinton, G., Hamilton, R.J., Raphael, R.A., Gonzalez, A.G., 1962. Hydrocarbon constituents of the wax coatings of plant leaves: a taxonomic survey. Nature 193, 739–742.
Farquhar, G.D., Ehleringer, J.R., Hubick, K.T., 1989. Carbon isotope discrimination and photosynthesis. Annu. Rev. Plant Physiol. Plant Mol. Biol. 40, 503–537.
Ficken, K.J., Barber, K.E., Eglinton, G., 1998. Lipid biomarker, δ13C and plant macrofossil stratigraphy of a Scottish montane peat bog over the last two millennia. Org. Geochem. 28, 217–237.
Fletcher, W.J., Sánchez Goñi, M.F., Allen, J.R.M., Cheddadi, R., Combourieu-Nebout, N., Huntley, B., Lawson, I., Londeix, L., Magri, D., Margari, V., Müller, U.C., Naughton, F., Novenko, E., Roucoux, K., Tzedakis, P.C., 2010. Millennial-scale variability during the last glacial in vegetation records from Europe. Quat. Sci. Rev. 29, 2839–2864.
Freeman, K.H., Pancost, R.D., 2013. Biomarkers for terrestrial plants and climate. In: Treatise on Geochemistry, second ed. Elsevier Inc, pp. 395–416.
Frost, D.R., 2015. Amphibian Species of the World: an Online Reference. Version 6.0. http://research.amnh.org/herpetology/amphibia/index.html. (Accessed November 2018).
Galván Santos, B., Hernández Gómez, C.M., Francisco Ortega, M.I., 2007. Elementos líticos apuntados en el Musteriense alcoyano. El Abric del Pastor (Alicante). Veleia 24–25, 367–383.
Garcin, Y., Schefuß, E., Schwab, V.F., Garreta, V., Gleixner, G., Vincens, A., Todou, G., Séné, O., Onana, J.-M., Achoundong, G., Sachse, D., 2014. Reconstructing C3 and C4 vegetation cover using n-alkane carbon isotope ratios in recent lake sediments from Cameroon, Western Central Africa. Geochem. Cosmochim. Acta 142, 482–500.
Gómez-Orellana, L., Ramil-Rego, P., Sobrino, C.M., 2007. The Würm in NW Iberia, a pollen record from area Longa (Galicia). Quat. Res. 67, 438–452.
Gunderson, L.H., 2000. Ecological resilience–in theory and application. Annu. Rev. Ecol. Systemat. 31, 425–439.
Hernández, F.J.M., Vinagre, A.T., Galván Santos, B., Hernández Gómez, C.M., 2010. Áreas de aprovisionamiento de sílex en el Paleolítico Medio en torno al Abric del Pastor (Alcoi, Alicante). Estudio macroscópico de la producción lítica de la colección Brotons. Recerques del Museu d'Alcoi 19, 65–80.
Hernández-Fernández, M., 2001. Bioclimatic discriminant capacity of terrestrial mammal faunas. Glob. Ecol. Biogeogr. 10, 189–204. https://doi.org/10.1046/j.1466-822x.2001.00218.x.
Hernández-Fernández, M., 2006. Rodent paleofaunas as indicators of climatic change in Europe during the last 125,000 years. Quat. Res. 65, 308–323. https://doi.org/10.1016/j.yqres.2005.08.022.
Hernández-Fernández, M., Peláez-Campomanes, P., 2003. The bioclimatic model: a method of palaeoclimatic. Glob. Ecol. Biogeogr. 12, 507–517. https://doi.org/10.1046/j.1466-822X.2003.00057.x.
Hijmans, R.J., Cameron, S.E., Parra, J.L., Jones, P.G., Jarvis, A., 2005. Very high-resolution interpolated climate surfaces for global land areas. Int. J. Climatol. 25, 1965–1978. https://doi.org/10.1002/joc.1276.

Holling, C.S., 1973. Resilience and stability of ecological systems. Annu. Rev. Ecol. Systemat. 4, 1–23.
IAEA/WMO, 2006. Global Network of isotopes in precipitation. Accessible at. In: The GNIP Database. http://www.iaea.org/water.
Jacquiot, C., Trenard, Y., Dirol, D., 1973. Atlas d'anatomie des bois des angiosperms (Essences feuillues). Centre Technique du Bois, Paris.
Jambrina-Enríquez, M., Sachse, D., Valero-Garcés, B.L., 2016. A deglaciation and Holocene biomarker-based reconstruction of climate and environmental variability in NW Iberian Peninsula: the Sanabria Lake sequence. J. Paleolimnol. 56, 49–66.
Jambrina-Enríquez, M., Recio, C., Vega, J.C., Valero-Garcés, B., 2017. Tracking climate change in oligotrophic mountain lakes: recent hydrology and productivity synergies in Lago de Sanabria (NW Iberian Peninsula). Sci. Total Environ. 590–591, 579–591.
Jambrina-Enríquez, M., Herrera-Herrera, A.V., Mallol, C., 2018. Wax lipids in fresh and charred anatomical parts of the Celtis australis tree: insights on paleofire interpretation. Org. Geochem. 122, 147–160.
Jeannet, M., 2000. Gruta da Figueira Brava: les rongeurs. Memorias da Academia das Ciências de Lisboa. Cl. Ciencias 38, 179–243.
Jiménez-Espejo, F.J., Martínez-Ruiz, F., Finlayson, C., Paytan, A., Sakamoto, T., Ortega-Huertas, M., Finlayson, G., Iijima, K., Gallego-Torres, D., Fa, D., 2007. Climate forcing and Neanderthal extinction in Southern Iberia: insights from a multiproxy marine record. Quat. Sci. Rev. 26, 836–852.
Jordan, S.F., Murphy, B.T., O'Reilly, S.S., Doyle, K.P., Williams, Grey A, Lee, S., McCaul, M.V., Kelleher, B.P., 2017. Mid-Holocene climate change and landscape formation in Ireland: evidence from a geochemical investigation of a coastal peat bog. Org. Geochem. 109, 67–76.
Kahmen, A., Schefuß, E., Sachse, D., 2013. Leaf water deuterium enrichment shapes leaf wax n-alkane δD values of angiosperm plants I: Experimental evidence and mechanistic insights. Geochem. Cosmochim. Acta 111, 39–49.
Kaplan, J.O., Colin Prentice, I., Buchmann, N., 2002. The stable carbon isotope composition of the terrestrial biosphere: modeling at scales from the leaf to the globe. Glob. Biogeochem. Cycles **16** (4), 8-1–8-11.
Kohn, M.J., 2010. Carbon isotope compositions of terrestrial C3 plants as indicators of (paleo) ecology and (paleo) climate. Proc. Natl. Acad. Sci. 107, 19691–19695.
Kreutzer, L.A., 1992. Bison and deer bone mineral densities: Comparisons and implications for the interpretation of archaeological faunas. J. Archaeol. Sci. 19, 271–294.
Kuder, T., Kruge, M.A., 1998. Preservation of biomolecules in sub-fossil plants from raised peat bogs - a potential paleoenvironmental proxy. Org. Geochem. 29, 1355–1368.
Lam, Y.M., Chen, X., Pearson, O.M., 1999. Intertaxonomic Variability in Patterns of Bone Density and the Differential Representation of Bovid, Cervid, and Equid Elements in the Archaeological Record. Am. Antiq. 64, 343–362.
Laplana, C., Sevilla, P., 2013. Documenting the biogeographic history of Microtus cabrerae through its fossil record. Mamm Rev. 43, 309–332. https://doi.org/10.1111/mam.12003.
Liu, J., An, Z., 2018. A hierarchical framework for disentangling different controls on leaf wax δDn-alkane values in terrestrial higher plants. Quat. Sci. Rev. 201, 409–417.
Liu, W., Yang, H., 2008. Multiple controls for the variability of hydrogen isotopic compositions in higher plant n-alkanes from modern ecosystems. Glob. Chang. Biol. 14, 2166–2177.
Liu, Z., Henderson, A.C.G., Huang, Y., 2008. Regional moisture source changes inferred from late holocene stable isotope records. Adv. Atmos. Sci. 25, 1021–1028.
López-García, J.M., Blain, H.A., Bennàsar, M., Sanz, M., Daura, J., 2013. Heinrich event 4 characterized by terrestrial proxies in southwestern Europe. Clim. Past 9, 1053–1064.
López-García, J.M., Blain, H.A., Bennàsar, M., Fernández-García, M., 2014. Environmental and climatic context of Neanderthal occupation in southwestern Europe during MIS3 inferred from the small-vertebrate assemblages. Quat. Int. 326–327, 319–328.
Lyman, R.L., 1984. Bone density and differential survivorship of fossil classes. J. Anthropol. Archaeol. 3, 259–299.
Lyman, R.L., 1985. Bone frequencies: differential transport, in situ destruction, and the MGUI. J. Archaeol. Sci. 12, 221–236. https://doi.org/10.1016/0305-4403(85)90022-6.
Lyman, R.L., 1994. Vertebrate Taphonomy; Cambridge Manuals in Archaeology. Cambridge University Press, Cambridge.
Machado, J., Hernández, C.M., Mallol, C., Galván Santos, B., 2013. Lithic production, site formation and Middle Palaeolithic palimpsest analysis: in search of human occupation episodes at Abric del Pastor Stratigraphic Unit IV (Alicante, Spain). J. Archaeol. Sci. 40, 2254–2273.
Machado, J., Mallol, C., Hernández, C.M., 2015. Insights into Eurasian Middle Palaeolithic settlement dynamics: the palimpsest problem. Settlement Dyn. of the Middle Paleolithic and Middle St. Age 4, 361e382.
Mallol, C., Hernández, C., Mercier, N., Falguères, C., Ben-Arous, E., Cabanes, D., Carrancho, A., Vidal-Matutano, P., Pérez, L., Connolly, R., Mayor, A., Galván, B., 2019. Fire and short-term human occupations in Iberia during MIS 4: Evidence from Abric del Pastor (Alcoy, Spain). Manuscript submitted for publication.
Marín-Arroyo, A.B., Rios-Garaizar, J., Straus, L.G., Jones, J.R., de la Rasilla, M., González Morales, M.R., Richards, M., Altuna, J., Mariezkurrena, K., Ocio, D., 2018. Chronological reassessment of the Middle to upper paleolithic transition and early upper paleolithic cultures in cantabrian Spain. PLoS One 13, e0194708.
Molina, F.J., Tarriño, A., Galván Santos, B., Hernández, C.M., 2010. Áreas de aprovisionamiento de sílex en el Paleolítico medio en torno al Abric del Pastor (Alcoi, Alicante), vol. 19. Recerques del Museu d'Alcoi.
Morales, J.V., Sanchis, A., 2009. The Quaternary fossil record of the genus Testudo in the Iberian Peninsula. Archaeological implications and diachronic distribution in the western Mediterranean. J. Archaeol. Sci. 36, 1152–1162. https://doi.org/10.1016/j.jas.2008.12.019.
Muñoz-Díaz, D., Rodrigo, F.S., 2004. Impacts of the North Atlantic Oscillation on the probability of dry and wet winters in Spain. Clim. Res. 27, 33–43.
Nabais, M., Zilhão, J., 2019. The consumption of tortoise among last interglacial iberian Neanderthals. Quat. Sci. Rev. https://doi.org/10.1016/j.quascirev.2019.03.024.
Nicosia, C., Stoops, G., 2017. Archaeological Soil and Sediment Micromorphology. John Wiley and Sons.
Norström, E., Norén, G., Smittenberg, R.H., Massuanganhe, E.A., Ekblom, A., 2018. Leaf wax δD inferring variable medieval hydroclimate and early initiation of Little Ice Age (LIA) dryness in southern Mozambique. Glob. Planet. Chang. 170, 221–233.
North Greenland Ice Core Project members, 2004. High-resolution record of Northern Hemisphere climate extending into the last interglacial period. Nature 431 (7005), 147–151, 9 September 2004.
Ochando, J., Carrión, J.S., Blasco, R., Fernández, S., Amorós, G., Munuera, M., Sañudo, P., Fernández Peris, J., 2019. Silvicolous Neanderthals in the far west: the mid-Pleistocene palaeoecological sequence of Bolomor Cave (Valencia, Spain). Quat. Sci. Rev. https://doi.org/10.1016/j.quascirev.2019.03.015.
Ortiz, J.E., Gallego, J.L.R., Torres, T., Díaz-Bautista, A., Sierra, C., 2010. Palaeoenvironmental reconstruction of Northern Spain during the last 8000 cal yr BP based on the biomarker content of the Roñanzas peat bog (Asturias). Org. Geochem. 41, 454–466.
Palomo, L.J., Gisbert, J., Blanco, J.C., 2007. Atlas y Libro Rojo de los Mamíferos Terrestres de Espana. Dirección General de Conservación de la Naturaleza, SECEM, SECEMU, Madrid.
Pérez, L., Sanchis, A., Hernández, C.M., Galván Santos, B., 2017. Paleoecología de macromamíferos aplicada a los conjuntos zooarqueológicos de El Salt y el Abric del Pastor (Alcoy, Alicante). In: Sanchis, A., Pascual, J.L. (Eds.), Interaccions entre felins i humans, 327–353. III Jornades d'arqueozoologia. Museu Prehistòria de València, Valencia.
Pita, R., Mira, A., Beja, P., 2014. Microtus cabrerae (rodentia: cricetidae). Mamm. Species 46 912, 48–70.
Poynter, J.G., Farrimond, P., Brassell, S.C., Eglington, G., 1989. Molecular Stratigraphic Study of Sediments from Holes 658A and 660A, Leg 108. Proceedings of the Ocean Drilling Program, Scientific Results 108, 387–394.
Rabeder, G., 1981. Die Arvicoliden (Rodentia, Mammalia) aus dem Pliozan und dem älteren Pleistozän von Niederösterreich. Beiträge zur Paläontologie Österreich 8, 1–373.
Reitz, E.J., Wing, E.S., 2008. Archaeological Theory and Methods, second ed. Cambridge University Press.
Reumer, J.W.F., 1984. Rusician and early Pleistocene soricidae (insectívora, mammalia) from tegelen (The Netherlands) and Hungary. Scr. Geol. 73, 1–173.
Rivas-Martínez, S., 1987. Memoria del mapa de series de vegetatción de España, vol. 1. I.C.O.N.A, Madrid, p. 400000.
Roček, Z., 1984. Lizards (reptilia: sauria) form the lower Miocene locality dolnice (bohemia, czechoslovakia). Rozpravy ceskoslovenské akademie věd. ř. mat. Přir. 94, 1–69.
Rodríguez, J., 2013. Paleoecología. In: Gracía-Díez, M., Zapata, L. (Eds.), Métodos y Técnicas de Análisis y Estudio en Arqueología Prehistórica: de lo técnico a la reconstrucción de los grupos humanos, 315–340. Servicio Editorial Argitalpen-Zerbitzua.
Sachse, D., Radke, J., Gleixner, G., 2006. δD values of individual n-alkanes from terrestrial plants along a climatic gradient–Implications for the sedimentary biomarker record. Org. Geochem. 37, 469–483.
Sachse, D., Kahmen, A., Gleixner, G., 2009. Significant seasonal variation in the hydrogen isotopic composition of leaf-wax lipids for two deciduous tree ecosystems (Fagus sylvativa and Acerpseudoplatanus). Org. Geochem. 40, 732–742.
Sachse, D., Billault, I., Bowen, G.J., Chikaraishi, Y., Dawson, T.E., Feakins, S.J., Freeman, K.H., Magill, C.R., McInerney, F.A., van der Meer, M.T.J., Polissar, P., Robins, R.J., Sachs, J.P., Schmidt, H.-L., Sessions, A.L., White, J.W.C., West, J.B., Kahmen, A., 2012. Molecular paleohydrology: interpreting the hydrogen-isotopic composition of lipid biomarkers from photosynthesizing organisms. Annu. Rev. Earth Planet Sci. 40, 221–249, 2012.
Sánchez Goñi, M.F., d'Errico, F., 2005. La historia de la vegetación y el clima del último ciclo climático (OIS5-OIS1, 140.000-10.000 años BP) en la Península Ibérica y su posible impacto sobre los grupos paleolíticos. Museo de Altamira, pp. 115–129. MONOGRAFÍAS no 20.
Sánchez Goñi, M.F., Eynaud, F., Turon, J., Shackleton, N.J., 1999. High resolution palynological record off the Iberian margin: direct land-sea correlation for the Last Interglacial Complex. Earth Planet. Sci. Lett. 171, 123–137.
Sánchez Goñi, M.F., Landais, A., Fletcher, W.J., Naughton, F., Desprat, S., Duprat, J., 2008. Contrasting impacts of Dansgaard–Oeschger events over a western European latitudinal transect modulated by orbital parameters. Quat. Sci. Rev. 27, 1136–1151.
Sánchez-Hernández, C., Rivals, F., Blasco, R., Rosell, J., 2014. Short, but repeated Neanderthal visits to Teixoneres Cave (MIS 3, Barcelona, Spain): a combined analysis of tooth microwear patterns and seasonality. J. Archaeol. Sci. 49, 317–325.

Sanchis, A., Morales, J.V., Pérez, L.J., Hernández, C.M., Galván Santos, B., 2015. La tortuga mediterránea en yacimientos valencianos del Paleolítico medio: distribución, origen de las acumulaciones y nuevos datos procedentes del Abric del Pastor (Alcoi, Alacant). In: Sanchis, A., Pasual, J.L. (Eds.), Preses petites i grups humans en el passat, 97–120. II Jornades d'arqueozologia. Museu Prehistòria de València, Valencia.
Schweingruber, F.H., 1976. Mikroskopische holzanatomic, Anatomie microscopique de bois. Birmensdorf: Institut féderal de recherches forestières, Zurcher AG.
Schweingruber, F.H., 1990. Anatomie Europäischer Hölzer. Bern (Haupt).
Stoops, G., 2003. Guidelines for Analysis and Description of Soil and Regolith Thin Sections. SSSA, Madison, WI.
Szyndlar, Z., 1984. Fossil snakes from Poland. Acta Zool. Cracov. 28, 1–156.
Tipple, B.J., Berke, M.A., Hambach, B., Roden, J.S., Ehleringer, J.R., 2015. Predicting leaf waxn-alkane2H/1H ratios: controlled water source and humidity experiments with hydroponically grown trees confirm predictions of Craig-Gordon model. Plant Cell Environ. 38 (6), 1035–1047.
Torres, T., Ortiz, J.E., Blázquez, A.M., Ruiz Zapata, B., Gil, M.J., Martín, T., Sánchez-Palencia, Y., 2015. The MIS 5 palaeoenvironmental record in the SE mediterranean coast of the iberian peninsula (río antas, almería, Spain). Clim. Past Discuss. 11, 3897–3936.
Uerpmann, H.P., 1973. Animal bone finds and economic archaeology: a critical study of Osteoarchaeological method. World Archaeol. 4, 307–322.
Uetz, P., Hošek, J., 2015. The Reptile Database. http://www.reptile-database.org. (Accessed November 2018).
Uno, K.T., Polissar, P.J., Kahle, E., Feibel, C., Harmand, S., Roche, H., deMenocal, P.B., 2016. A Pleistocene palaeovegetation record from plant wax biomarkers from the Nachukui Formation, West Turkana, Kenya. Philos. Trans. R. Soc. Lond. B Biol. Sci. 371.
van der Meulen, A., 1973. Middle Pleistocene smaller mammals from the montepeglia (orvieto, Italy), with special reference to the phylogeny of Microtus (arvicolidae, rodentia). Quaternaria 17, 1–144.
van der Weerd, A., 1976. Rodents Faunas of the Mio-Pliocene Sediments of the Teruel-Alfambra Region, vol. 2. Utrecht Micropaleontological Bulletins Special Publication, Spain, pp. 1–217.
Vidal-Matutano, P., Hernández, C.M., Galván Santos, B., Mallol, C., 2015. Neanderthal firewood management: evidence from Stratigraphic Unit IV of Abric del Pastor (Eastern Iberia). Quat. Sci. Rev. 111, 81–93.
Vidal-Matutano, P., Henry, A., Théry-Parisot, I., 2017. Dead wood gathering among Neanderthal groups: charcoal evidence from Abric del Pastor and El Salt (Eastern Iberia). J. Archaeol. Sci. 80, 109–121.
Vliet-Lanoë, B.V., 2010. Frost action. In: Stoops, G., Marcelino, V., Mees, F. (Eds.), Interpretation of Micromorphological Features of Soils and Regoliths, 81–108. Elsevier, Amsterdam.
Walter, H., 1973. Vegetation of the Earth. The English University Press, London.
Wang, X., Huang, X., Sachse, D., Ding, W., Xue, J., 2016. Molecular paleoclimate reconstructions over the last 9 ka from a peat sequence in south China. PLoS One 11, e0160934.
Wang, C., Eley, Y., Oakes, A., Hren, M., 2017. Hydrogen isotope and molecular alteration of n-alkanes during heating in open and closed systems. Org. Geochem. 112, 47–58.
Wiesenberg, G.L.B., Lehndorff, E., Schwark, L., 2009. Thermal degradation of rye and maize straw: lipid pattern changes as a function of temperature. Org. Geochem. 40, 167–174.
Wilson, D.E., Reeder, D.M., 2005. Mammal Species of the World: a Taxonomic and Geographic Reference. Johns Hopkins University Press, Baltimore.
Wolf, D., Kolb, T., Alcaraz-Castaño, M., Heinrich, S., Baumgart, P., Calvo, R., Sánchez, J., Ryborz, K., Schäfer, I., Bliedtner, M., Zech, R., Zöller, L., Faust, D., 2018. Climate deteriorations and Neanderthal demise in interior Iberia. Sci. Rep. 8, 7048.
Wood, R.E., Barroso-Ruíz, C., Caparrós, M., Jordá Pardo, J.F., Galván Santos, B., Higham, T.F.G., 2013. Radiocarbon dating casts doubt on the late chronology of the Middle to Upper Palaeolithic transition in southern Iberia. Proc. Natl. Acad. Sci. U. S. A. 110, 2781–2786.
Wu, M., Zhuang, G., Hou, M., Miao, Y., 2018. Ecologic shift and aridification in the northern Tibetan Plateau revealed by leaf wax n-alkane δ2H and δ13C records. Palaeogeogr. Palaeoclimatol. Palaeoecol. 514, 464–473.
Xie, S., Nott, C.J., Avsejs, L.A., Maddy, D., Chambers, F.M., Evershed, R.P., 2004. Molecular and isotopic stratigraphy in an ombrotrophic mire for paleoclimate reconstruction. Geochem. Cosmochim. Acta 68, 2849–2862.
Yang, H., Huang, Y., 2003. Preservation of lipid hydrogen isotope ratios in Miocene lacustrine sediments and plant fossils at Clarkia, northern Idaho, USA. Org. Geochem. 34, 413–423.